Parabolic and Non-Parabolic Surfaces with Small or Large End Spaces via Fenchel-Nielsen Parameters

by

MICHAEL ANTONY PANDAZIS

A dissertation submitted to the Graduate Faculty in Mathematics in partial fulfillment of the requirements for the degree of Doctor of Philosophy, The City University of New York

2024

APPROVAL

Parabolic and Non-Parabolic Surfaces with Small or Large End Spaces via Fenchel-Nielsen Parameters

by

Michael Antony Pandazis

This manuscript has been read and accepted for the Graduate Faculty in Mathematics in satisfaction of the thesis requirement for the degree of Doctor of Philosophy.

Approved: April, 2024

Dragomir Šarić, Advisor and Defense Committee Member
Ara Basmajian, Defense Committee Member
Enrique Pujals, Defense Committee Member
Christian Wolf, Executive Officer

THE CITY UNIVERSITY OF NEW YORK

ABSTRACT

Parabolic and Non-Parabolic Surfaces with Small or Large End Spaces via Fenchel-Nielsen Parameters

by

Michael Antony Pandazis

Advisor: Dragomir Šarić

A Riemann surface supports a unique conformal hyperbolic metric. The geodesic flow considered in the thesis is for this hyperbolic metric. A *Green's function* on X is a harmonic function u with the logarithmic singularity at a single point $z_0 \in X$ such that $\lim_{z\to\partial X} u(z) = 0$ ([3]). If X does not support a Green's function, it is said to be *parabolic*; otherwise, it is *non-parabolic* (see Ahlfors-Sario [3]). A Riemann surface is parabolic if and only if the geodesic flow on its unit tangent bundle is ergodic. When the covering group of X is of the first kind, any topological pants decomposition is homotopic to a geodesic pants decomposition. To each cuff, i.e.-a boundary component of a pair of pants, there is associate length and twist. The lengths and twists on all cuffs, called the Fenchel-Nielsen parameters, uniquely determine the Riemann surface X. Conversely, given an assignment of lengths and twists on all cuffs, there exists a unique Riemann surface that realizes them.

A Riemann surface with countably many punctures that accumulate to a single topological end is called a *flute surface* (see [6]). Consider a fixed standard geodesic pants decomposition of a flute. When the twist on every cuff is one-half, it is called a half-twist flute. A Riemann surface is *symmetric* (with respect to a pants decomposition) if there is an orientation reversing isometry that permutes the right-angled hexagon decomposition of each pair of pants.

Every flute surface with only zero or half twists is symmetric. We prove that a symmetric flute surface with only zero or half-twists is parabolic if and only if its Fuchsian covering

group is of the first kind. That equivalence simplifies the problem of determining whether or not a half-twist flute is parabolic using its Fenchel-Nielsen coordinates.

Results we obtain in the thesis concerning whether or not half-twist flutes are parabolic using their Fenchel-Nielsen coordinates extend what was already proved by Basmajian, Hakobyan, and Šarić ([7]). They successfully characterized the parabolicity of half-twist flutes with concave length parameters. In the thesis, we do not assume the length parameters are concave, thus completing the problem of determining the parabolicity of half-twist flutes using their Fenchel-Nielsen coordinates.

Moreover, we study another interesting class of surfaces. Consider a compact exhaustion X_n of a surface X by geodesic subsurfaces. An *end* of X is represented by a decreasing sequence of connected sets C_n such that C_n is a connected component of $X - X_n$. We say such an end is *accumulated by genus* if each C_n corresponding to the end has positive genus. A Riemann surface X with finitely many ends accumulated by genus is *end symmetric* if each end surface, which is a bordered surface with one closed geodesic on its boundary and one topological end, is symmetric in the above sense. We obtain that an end symmetric Riemann surface X, such that the cuff lengths of attached genus is bounded, is parabolic if and only if it has a Fuchsian covering group of the first kind. Using that result, we find conditions on the Fenchel-Nielsen coordinates of X that determine whether or not X is parabolic.

The *Cantor tree surfaces* are infinite Riemann surfaces with a Cantor set of ends. In this thesis we obtain that Cantor tree surfaces are non-parabolic if their length parameters along every end are between two rates of convergence to zero. Consider two geodesic pair of pants attached via a single cuff. The result is a level one surface X_1. Attach to each geodesic boundary of X_1 a pair of pants to obtain the surface X_2. The attached pairs of pants constitute level two of the surface. Continue in this fashion indefinitely to obtain the Cantor tree surface X and a compact exhaustion X_n of X. The *level n pants of X* are the pairs of pants in the decomposition of the subsurface X_n of X that are adjacent to the boundary of X_n for $n \geq 1$. We call the boundary cuffs of X_n the *level n cuffs* for $n \geq 1$. To make a new class of surfaces, insert between each level n cuff a surface with two geodesic boundaries

and genus at most C. One can also choose not to insert anything. Redefine the level n cuffs to be the cuff between an inserted surface and a level $n+1$ pair of pants. Assume the lengths of cuffs are decreasing along each end. The result is a *blooming Cantor tree surface* $\tilde{X}$. We obtain that $\tilde{X}$ is not parabolic if its length parameters converge rapidly to zero along every end. The thesis extends the result attained by Šarić ([18]) that X is non-parabolic when the lengths of cuffs converge slower to infinity, and complements the result obtained by Basmajian, Hakobyan, and Šarić ([7]) in proving that $\tilde{X}$ is parabolic when the lengths of level n cuffs are small.

ACKNOWLEDGMENTS

Thank you to my advisor Dragomir Šarić, whose guidance, advice, and support shaped and sustained this project. Also, thank you to Dragomir Šarić, Ara Basmajian, and Enrique Pujals for being on my defense committee.

TABLE OF CONTENTS

LIST OF FIGURES

LIST OF APPENDICES

Chapter 1

Introduction

A Riemann surface X is *infinite* if its fundamental group cannot be finitely generated. Recall that a *Green's function* on X is a harmonic function u with the logarithmic singularity at a single point $z_0 \in X$ such that $\lim_{z\to\partial X} u(z) = 0$ ([3]). If X does not support a Green's function, it is said to be *parabolic*; otherwise, it is *non-parabolic* (see Ahlfors-Sario [3]). The classification of surfaces as parabolic and non-parabolic is pertinent since a large number of equivalent conditions are found in many diverse fields of mathematics (see [3], [5], [10], [12], [14], [15], [20], [21], [1], [22], and [18]). The following is a partial list of conditions that are equivalent to the parabolicity of $X = \mathbb{H}/\Gamma$:

1. the geodesic flow on the unit tangent bundle $T^1(X)$ of X is ergodic,
2. the Poincaré series $\sum_{\gamma\in\Gamma} e^{-d_h(z,\gamma(z))}$ is divergent, where $X = \mathbb{H}/\Gamma$, $d_h(.,.)$ is the hyperbolic distance in $\mathbb{H}$ and $z \in \mathbb{H}$,
3. the harmonic measure of the ideal boundary with respect to any compact subsurface vanishes,
4. the Brownian motion on X is recurrent,
5. the surface X does not support a non-constant positive subharmonic function,
6. given any compact $K \subset X$ and the set $\mathscr{F}$ of all differentiable curves from K to the boundary at infinity of X, the extremal length of $\mathscr{F}$ is infinite,

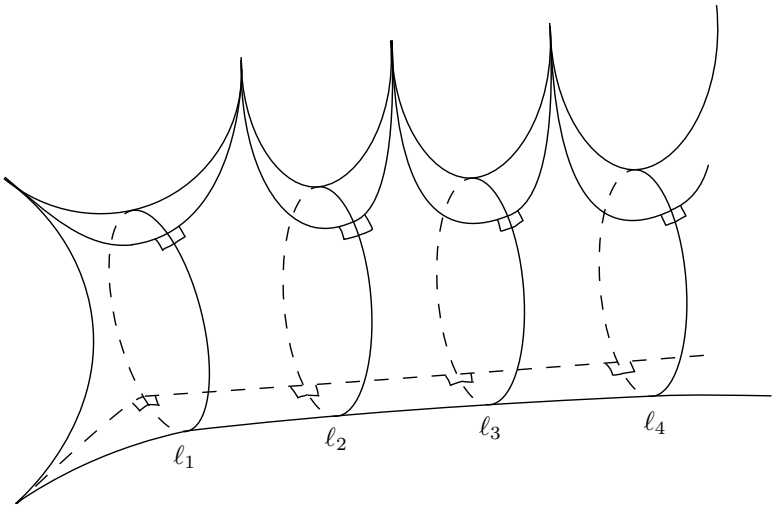

Figure 1.1: The zero twist flute surface.

7. the group Γ has the Bowen property.

A *topological pair of pants* is homeomorphic to a sphere minus three closed disks. If the boundary components of a topological pair of pants are straightened into simple closed geodesics, then the result is a *geodesic pair of pants*. A *topological pants decomposition* of a surface is a locally finite decomposition into pairs of pants such that the boundary curves are non-trivial and homotopically distinct. By [16], every infinite Riemann surface has a topological pants decomposition. When the pairs of pants in a topological pants decomposition of a surface are all straightened into geodesic pairs of pants, one obtains a *geodesic pants decomposition*.

Consider a fixed geodesic pair of pants with two cusps and one simple closed geodesic boundary. Attach in an infinite chain geodesic pairs of pants with two simple closed geodesic boundaries and one cusp. The result is a *tight flute surface* X_f. When every twist is zero, it is called a *zero-twist flute* X_f^0 (see Figure 1.1). The simple closed geodesics between attached pairs of pants are called *cuffs*. The union of the first n pairs of pants is a geodesic subsurface X_n. These X_n make up a compact exhaustion of X. Denote the geodesic boundary of X_n by α_n and its length by $l_n = l(\alpha_n)$. Basmajian, Hakobyan, and Šarić ([7]) obtained a complete characterization of zero-twist flutes. They found that X_f^0 is parabolic if and only if X_f^0 has Fuchsian covering group of the first kind if and only if $\sum_{n=1}^{\infty} e^{-\frac{l_n}{2}} = \infty$.

A *symmetric surface* is a surface with a pants decomposition consisting of pants that have both a front and a back hexagon that are interchanged by an orientation-reversing isometry of the surface. A flute surface with only zero or half twists is symmetric.

We simplify the problem of determining whether or not symmetric flutes are parabolic using their Fenchel-Nielsen coordinates with the following theorem.

Theorem 1.1. *Let $X_f = \mathbb{H}/\Gamma$ be a flute surface with $t_n \in \{0, 1/2\}$ for $n \geq 1$. Then X_f is parabolic if and only if Γ is of the first kind.*

Consider a compact exhaustion X_n of X. An *end* of X is represented by a decreasing sequence of connected sets C_n such that C_n is a connected component of $X - X_n$. We say such an end is *accumulated by genus* if each C_n corresponding to the end has positive genus. A Riemann surface X with finitely many ends accumulated by genus is *end symmetric* if each end surface, which is a bordered surface with one closed geodesic boundary and one topological end, is symmetric in the above sense. For each end surface, let β_n be cuffs that cut off a genus one surface with geodesic boundary, and let α_n be closed geodesics that accumulate toward the infinite end. In each torus cut off by β_n, we add another simple closed geodesic γ_n. We simplify the problem of determining the parabolicity of end symmetric surfaces with the following theorem.

Theorem 1.2. *Let $X = H/\Gamma$ be a Riemann surface that is end symmetric with the lengths $\ell(\beta_n)$ and $\ell(\gamma_n)$ between two positive constants. Then X is parabolic if and only if Γ is of the first kind.*

A *half-twist flute*, denoted by $X_f^{\frac{1}{2}}$, is a flute surface with only half twists. Consider a compact exhaustion X_n of a half-twist flute $X = X_f^{\frac{1}{2}}$. Basmajian, Hakobyan, and Šarić ([7]) used the countable sum of the moduli of the union of two non-standard half-collars to obtain if

$$\sum_{n=1}^{\infty} e^{-\frac{\ell_n}{4}} = \infty \tag{1.1}$$

then $X_f^{\frac{1}{2}}$ is parabolic. If the length parameters ℓ_n are increasing and concave, then condition (1.1) is equivalent to both $X_f^{\frac{1}{2}}$ being parabolic and Γ being of the first kind. Define $\sigma_n =$

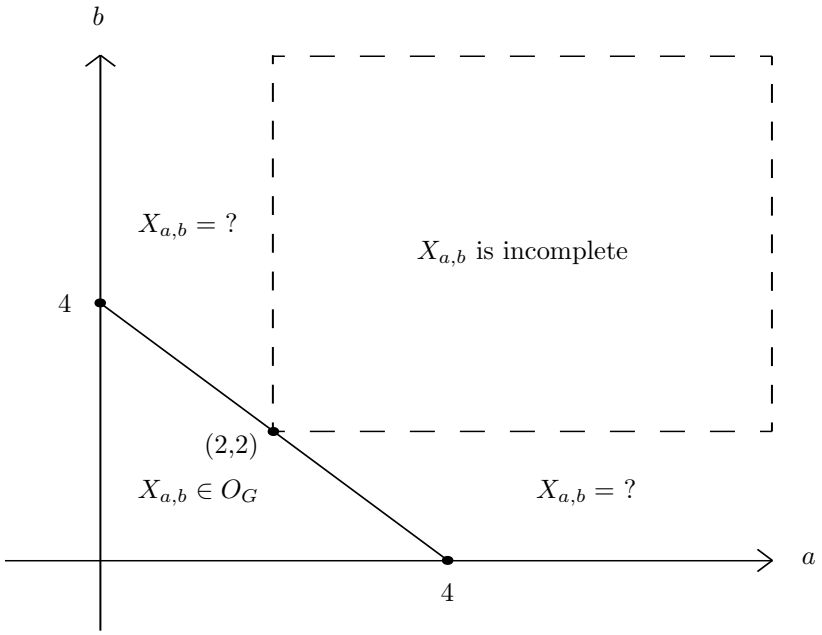

Figure 1.2: A slice of flutes $X_{a,b}$.

$\ell_n - \ell_{n-1} + \ell_{n-2} - \ell_{n-3} + ... + (-1)^{n-1}\ell_1$ for $n \geq 1$.

If

$$\sum_{n=1}^{\infty} e^{-\frac{\sigma_n}{2}} < \infty, \tag{1.2}$$

then $X_f^{\frac{1}{2}}$ is incomplete and thus non-parabolic ([7]).

To illustrate the difference between (1.1) and (1.2), we define the *Hakobyan slice* (see [7], Example 9.9). For any positive values of a and b, define the length parameters of a half-twist flute $X = X_{a,b}$ by

$$\ell_{2n} = a\ln(n+1) + b\ln(n), \qquad \ell_{2n+1} = (a+b)\ln(n+1)$$

for $n \geq 1$ (see Figure 1.2). The length parameters of $X_{a,b}$ are increasing but non-concave. When $a + b \leq 4$, condition (1.1) is satisfied, and $X_{a,b}$ is parabolic. For values of a and b such that $min\{a, b\} > 2$, condition (1.2) is satisfied, and $X_{a,b}$ is incomplete and thus non-parabolic. It was an open question as to whether or not $X_{a,b}$ is parabolic when neither condition (1.1) nor (1.2) is met (see Figure 1.2). Moreover, a complete characterization of the parabolicity of half-twist flutes was missing.

Theorem 1.3. *Assume that the lengths ℓ_n of the boundary geodesics of the pants decomposition of a half-twist flute surface $X_f^{1/2} = \mathbb{H}/\Gamma$ are increasing. Then the following are equivalent.*

- *the covering group Γ of $X_f^{1/2}$ is of the first kind,*
- *$\sum_{n=1}^{\infty} e^{-\frac{\sigma_n}{2}} = \infty$, and*
- *$X_f^{1/2}$ is parabolic.*

Using Theorem 1.3, we determine whether or not each half-twist flute $X_{a,b}$ in the Hakobyan slice is parabolic.

Theorem 1.4. *In the slice $X_{a,b}$ above, the Riemann surface $X_{a,b}$ has Fuchsian covering group of the second kind if and only if $\min\{a,b\} > 2$. Moreover, $X_{a,b}$ is parabolic if and only if $\min\{a,b\} \leq 2$.*

We give a complete characterization of whether or not a special class of end symmetric surfaces with only half twists in each end is parabolic with the following theorem.

Theorem 1.5. *Let X be a Riemann surface with finitely many ends whose twists are $1/2$ on the simple closed geodesics α_n accumulating at each end. Assume that the lengths $\ell(\beta_n)$ and $\ell(\gamma_n)$ are between two positive constants. Let ℓ_n be the length of α_n and assume that ℓ_n is increasing. Then the following are equivalent.*

1. *the covering group Γ of X is of the first kind,*
2. *$\sum_{n=1}^{\infty} e^{-\frac{\sigma_n}{2}} = \infty$ for each end X_i, and*
3. *X is parabolic.*

Let X_C be a *Cantor tree surface* equipped with a geodesic pants decomposition (see Figure 1.3). At level n of the surface X_C, there are 2^n pairs of pants, and the union of all pairs of pants up to and including level n pants is a compact subsurface X_n with 2^{n+1} geodesic boundaries (see Figure 1.3). The *level n geodesics* are the geodesic boundary components of X_n. Basmajian, Hakobyan, and Šarić [7, Theorem 10.3] obtained that the surface X_C admits

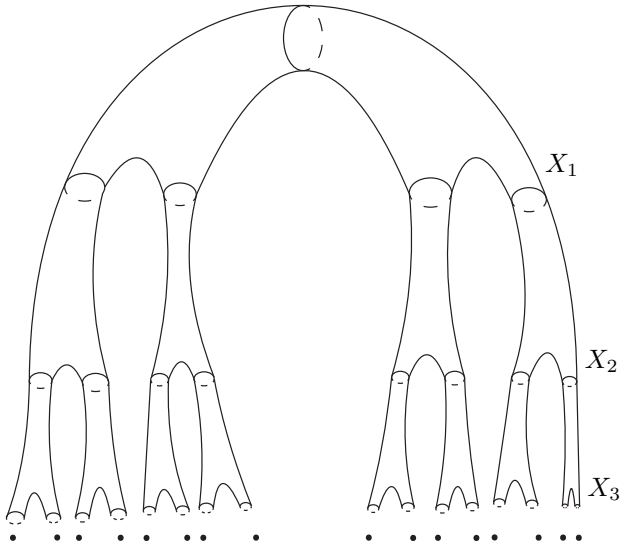

Figure 1.3: The Cantor tree surface with a geodesic pants decomposition.

no Green's function if each boundary geodesic α_n at the level n has its length bounded above by $\frac{n}{2^n}$. Since the proof of [7, Theorem 10.3] only relies on standard half collars around the simple closed geodesics α_n that conclusion still applies to the blooming Cantor trees. Note that this theorem implies the same statement is true if we replace n with n^r for any fixed $r \leq 1$. Using that it has numerous ends, McMullen [13] proved if every boundary geodesic of the pants decomposition of X_C has its length between two positive constants, then X_C is not parabolic. More recently, Šarić [18, Theorem 4.1] proved that X_C is not parabolic if the lengths of level n geodesics are $\frac{n^r}{2^n}$ for $r > 2$. From a result in [4], we can consider X_C with zero twists because twisting along geodesics of bounded length is a quasiconformal deformation that preserves parabolicity.

We consider the Cantor tree surfaces with lengths of level n geodesic boundaries l_n that satisfy for any fixed $r > 1$, the inequalities $C_1 \frac{n^r}{2^n} \leq l_n \leq \frac{C_2}{n^2}$ for some constants $C_1, C_2 > 0$. That condition is between the case considered by Basmajian, Hakobyan, and Šarić when $\ell_n \leq \frac{n}{2^n}$ and the case $\ell_n = \frac{n^r}{2^n}$ for $r > 2$ considered by Šarić.

Theorem 1.6. *Let X be the Cantor tree surface, as depicted in Figure 1.3. Let l_n^j be the lengths of the geodesic boundaries α_n^j of X_n for $n \geq 1$ and for $1 \leq j \leq 2^{n+1}$. If there is an*

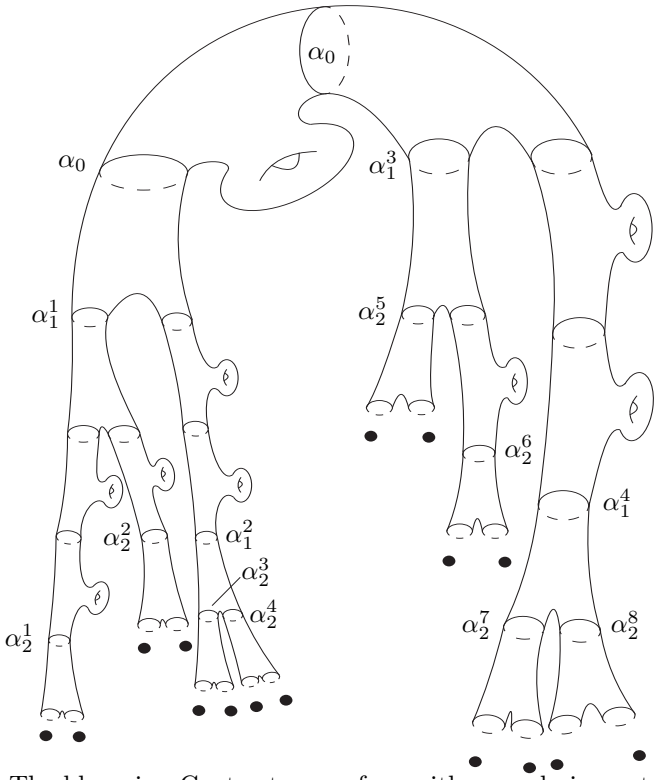

Figure 1.4: The blooming Cantor tree surface with a geodesic pants decomposition.

$r > 1$ such that

$$C_1 \frac{n^r}{2^n} \leq l_n^j \leq \frac{C_2}{n^2}$$

for some universal constants $C_1, C_2 > 0$, then X is not parabolic.

Our methods extend to surfaces with infinite genus and a Cantor set of ends called *blooming Cantor trees* (see Figure 1.4). We define the blooming Cantor tree surface $\tilde{X}$ by a construction starting with a Cantor tree X. Fix a geodesic pants decomposition of X. Consider the 2^n many level n pairs of pants in X as depicted in Figure 1.4. The union of all pairs of pants up to and including the level n pairs of pants constitute the geodesic subsurface X_n of X. For any n, we insert between each of the geodesic boundaries of X_n and a level $n+1$ pair of pants a subsurface with genus at most C and two geodesic boundaries. Redefine α_n as the cuff between the inserted subsurface and a level $n+1$ pair of pants. The cuff lengths are decreasing along the inserted subsurface.

Theorem 1.7. *Consider the blooming Cantor tree surface $\tilde{X}$ depicted in Figure 1.4. Let l_n^j be the lengths of the geodesic boundaries α_n^j of X_n for $n \geq 1$ and for $1 \leq j \leq 2^{n+1}$. If, for*

some $r > 1$ and some positive constants C_1 and C_2,

$$C_1 \frac{n^r}{2^n} \leq l_n^j \leq \frac{C_2}{n^2},$$

then $\tilde{X}$ is not parabolic.

Chapter 2

Geodesic Pants Decomposition of a Riemann surface

A Riemann surface is *infinite* if its fundamental group cannot be finitely generated. An infinite Riemann surface supports a unique hyperbolic metric in its conformal class, and it is isometric to $\mathbb{H}/\Gamma$, where $\mathbb{H}$ is the hyperbolic plane, and Γ is a Fuchsian covering group.

A *topological pair of pants* is homeomorphic to a sphere with three closed disks removed. The boundaries of these disks are sometimes considered part of a pair of pants. If the boundary components of a topological pair of pants get straightened into simple closed geodesics, one has a *geodesic pair of pants*. A geodesic pair of pants with one or two cusps as boundary components is called a *tight pair of pants*.

We define a *topological pants decomposition* of a surface as a locally finite decomposition into pairs of pants where the boundary curves are homotopically distinct and non-trivial. Every Riemann surface is triangulable. By [16], any triangulable infinite Riemann surface has a topological pants decomposition. When the pairs of pants in a topological pants decomposition of a surface are all geodesic pairs of pants; the separation is called a *geodesic pants decomposition*.

The *convex core* of a Riemann surface is the minimal closed convex subsurface with boundary that carries all the homotopy. The Riemann surface is the result of attaching

hyperbolic funnels to closed geodesics on the boundary of the convex core and by attaching geodesic half-planes to open boundary geodesics of the convex core. Let $X = \mathbb{H}/\Gamma$ be a Riemann surface. The covering Fuchsian group Γ is said to be *of the first kind* if the limit set of Γ is equal to the ideal boundary of $\mathbb{H}$. Otherwise, it is said to be *of the second kind*.

Chapter 3

Fenchel-Nielsen Parameters of a Riemann surface

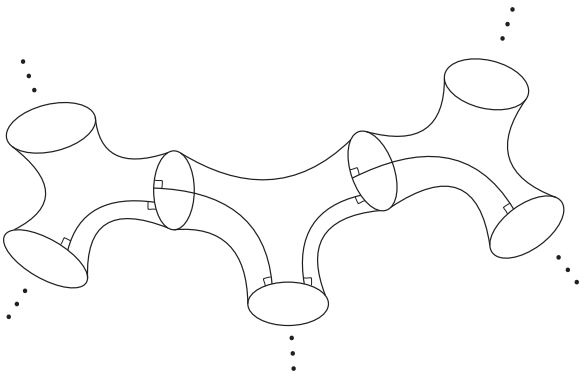

Figure 3.1: Length and twist parameters are associated with each closed geodesic boundary of a fixed geodesic pants decomposition of a surface.

Every topological pants decomposition of a surface can get straightened into a geodesic pants decomposition. Fix a geodesic pants decomposition of a Riemann surface X. We associate with each simple closed geodesic boundary of this decomposition its length, called a *length parameter*. We also associate with it a *twist parameter*, which is the relative hyperbolic distance between feet of orthogeodesics from the nearest closed geodesics on both sides. The length and twist parameters constitute the *Fenchel-Nielsen parameters* of a Riemann surface associated with a fixed geodesic pants decomposition (see Figure 3.1).

Chapter 4

Parabolic surfaces, modulus, and extremal length

Let X be a Riemann surface. A *Green's function* on X is a harmonic function u on X with the logarithmic singularity at a single point of X such that $lim_{z\to\partial X}u(z) = 0$ ([3]). We say a Riemann surface is *parabolic* if it does not admit a Green's function ([3]). *The type problem for Riemann surfaces* is determining when an explicit construction gives rise to a Riemann surface that does not admit a Green's function.

The Liouville measure is invariant under geodesic flow. To effectively study the behavior of geodesic flow, one should study the Liouville measure. Let g be the geodesic flow on the unit tangent bundle of X. We say g is *ergodic* if for any $g-$invariant set A, either the Liouville measure of A is zero or of its complement is zero. The property of parabolicity for a Riemann surface is equivalent to the geodesic flow being ergodic and the Poincare series being divergent.

A *metric* ρ on X is a non-negative Borel-measurable function defined on X. It allows the definition of distances and angles. A manifold equipped with such a metric is a Riemannian manifold. Let Γ be a family of curves on X. A metric ρ is *allowable* for Γ if the ρ length of every curve γ in Γ is at least one. The ρ length of non-rectifiable curves are assumed infinite.

Definition 4.1. The *modulus* of a curve family Γ, denoted by $mod\Gamma$, is

$$\text{mod}\Gamma = \inf_{\rho} \iint_X \rho^2(z)dxdy$$

where the infimum is over all allowable metrics ρ for Γ.

Below is a list of relevant properties of the modulus of curve families.

Lemma 4.2. *Let $\{\Gamma_n\}_{n=1}^{\infty}$ be a sequence of curve families. Then the following properties apply.*

- *If $\Gamma_i \subset \Gamma_j$, then* $\text{mod}\Gamma_i \leq \text{mod}\Gamma_j$
- $\text{mod}(\cup_{n=1}^{\infty}\Gamma_n) \leq \sum_{n=1}^{\infty} \text{mod}\Gamma_n$
- *If $\Gamma_i < \Gamma_j$, then* $\text{mod}\Gamma_i \geq \text{mod}\Gamma_j$

where $\Gamma_i < \Gamma_j$ is read "Γ_i minorizes Γ_j" and means that for every curve γ_j in Γ_j, there exists a curve γ_i in Γ_i such that $\gamma_i \subset \gamma_j$. The first property is called *monotonicity*, the second property is called *subadditivity*, and the third is called the *overflowing* property. When the sequence of curve families is pairwise disjoint, the inequality in the subadditivity property becomes equality.

To determine the parabolicity of Riemann surfaces, we use what is known as the modular test. Let $\{X_n\}$ be a compact exhaustion of X such that $\bar{X_n} \subset X_{n+1}$. Denote the boundary of X_n by β_n. Let $\lambda_{X_n - X_1}(\beta_1, \beta_n)$ be the *extremal distance* between β_1 and β_n in $X_n - X_1$, where the extremal distance is the reciprocal of the modulus of the curve family connecting β_1 and β_n in $X_n - X_1$.

Proposition 4.3 ([3], page 229)**.** The Riemann surface X is parabolic if and only if

$$\lambda_{X_n - X_1}(\beta_1, \beta_n) \to \infty$$

as $n \to \infty$.

Chapter 5

Symmetric surfaces and the modulus of curve families

We focus our attention on surfaces with symmetry, as defined below.

Definition 5.1. An infinite Riemann surface X is said to be *symmetric* if there exists an orientation-reversing isometry (anti-conformal reflection) $R : X \to X$ where the fixed points are a collection of pairwise disjoint bi-infinite and/or closed geodesics that divide the surface into two connected components permuted by R.

Let R_f be the set of fixed points of an orientation-reversing isometry on a symmetric surface X. The set R_f separates X into two symmetric halves. We choose either side and call it the *front* side $X^\star$, while the other side is called the *back* side $X^{\star\star}$.

We establish an asymptotic comparison between the modulus of curve families in X to the modulus of curve families in $X^\star$. This will give necessary and sufficient conditions for the parabolicity of symmetric surfaces.

Theorem 5.2. *Consider an infinite symmetric Riemann surface X with an orientation reversing isometry $R : X \to X$. Let $\{X_n\}_{n=1}^{\infty}$ be an exhaustion of X by finite area subsurfaces with compact geodesic boundary that are invariant under R. Denote by Γ_n the family of curves that connects ∂X_1 and ∂X_n inside $X_n \setminus X_1$. Let $\Gamma_n^\star$ be the subfamily of Γ_n that lies in the*

front side $X^\star$ of $X \setminus f(R)$. Then

$$\lim_{n\to\infty} \mathrm{mod}\Gamma_n = 0$$

if and only if

$$\lim_{n\to\infty} \mathrm{mod}\Gamma_n^* = 0.$$

Proof. Since $\Gamma_n^\star \subset \Gamma_n$, by the monotonicity property of modulus, $\mathrm{mod}\ \Gamma_n^\star \leq \mathrm{mod}\ \Gamma_n$. Thus, one direction of the proof is immediate. Now assume $\lim_{n\to\infty} \mathrm{mod}\Gamma_n^\star = 0$ to deduce that $\lim_{n\to\infty} \mathrm{mod}\Gamma_n = 0$. That gives us a sequence of allowable metrics $\rho_n^\star$ on $X_n^\star$ such that

$$\mathrm{mod}\Gamma_n^\star = \iint_{X_n^\star} {\rho_n^\star}^2(z)dxdy \to 0$$

as $n \to \infty$. Define the sequence of metrics ρ_n on X_n in the following way. For z in $X^\star$, define $\rho_n(z) = \rho_n^\star(z)$. If z belongs to the set R_f, let $\rho_n(z)$ be infinite. Define $\rho_n(z) = \rho_n^\star(R(z))$ for every z in $X^{\star\star}$.

We show that ρ_n is an allowable metric for X_n. If a curve γ lies entirely inside $X_n^\star$, then $\ell_{\rho_n}(\gamma) = \ell_{\rho_n^\star}(\gamma) \geq 1$. Moreover, if a curve γ intersects R_f on a set of positive measure, then $\ell_{\rho_n}(\gamma)$ is infinite. Also, if γ is not in $X_n^\star$, and it does not intersect R_f on a set of positive measure, reflect every maximal sub curve of γ in $X_n^{\star\star}$ by R to $X_n^\star$. Then $\ell_{\rho_n}(\gamma) = \ell_{\rho_n^\star}(\gamma) \geq 1$. That implies ρ_n is allowable for X_n.

Thus, we obtain that

$$\mathrm{mod}\Gamma_n = \iint_{X_n} \rho_n^2(z)dxdy = 2\iint_{X_n^\star} {\rho_n^\star}^2(z)dxdy$$

and the rest of the proof is immediate. □

Chapter 6

The equivalence of parabolicity and completeness for symmetric surfaces

A Riemann surface X with the induced metric is *complete* if and only if its Fuchsian covering group is of the first kind. There exist surfaces that have Fuchsian covering groups of the first kind that are not parabolic. McMullen proved that Cantor tree surfaces are non-parabolic when their geodesic boundaries have lengths between two positive constants. Thus, it is interesting to consider symmetric surfaces in which parabolicity and completeness are equivalent.

6.1 The zero-twist flute

Consider a fixed geodesic pair of pants with two cusps and one geodesic boundary. Attach in an infinite chain geodesic pair of pants with two boundary geodesics and one cusp. The result is a *flute* surface. A flute surface with all zero twists is called a *zero-twist flute*.

The twist parameters are crucial to solve the type problem when the surface has a small set of ends and large lengths. Basmajian, Hakobyan and Šarić proved the following theorem in such a circumstance.

Theorem 6.1 ([7])**.** *Let X be a tight flute surface with the Fenchel-Nielsen coordinates*

$\{(\ell_n, t_n)\}_n$ *which correspond to the closed geodesics* α_n *on the boundary of the pants decomposition.*

If

$$\sum_{n=1}^{\infty} e^{-\frac{\ell_n}{2}} = \infty$$

or

$$\sum_{n=1}^{\infty} e^{-(1-|t_n|)\frac{\ell_n}{2}} = \infty$$

then X *is parabolic.*

Moreover, they obtained a complete characterization of the parabolicity and completeness of zero-twist flutes.

Theorem 6.2 ([7])**.** *Let* X *be a flute surface with twists* $t_n = 0$ *for* $n \geq 1$*. Then the following are equivalent.*

- $X = \mathbb{H}/\Gamma$ *has the covering group* Γ *of the first kind,*
- $\sum_{n=1}^{\infty} e^{-\frac{\ell_n}{2}} = \infty$ *and*
- X *is parabolic.*

6.2 The half-twist flute

When all the twists of a flute surface are $\frac{1}{2}$, it is called a *half-twist flute*. For half-twist flutes with increasing and concave length parameters, [7] proved completeness and parabolicity are equivalent. That conclusion was missing without concave length parameters. Using new methods, we obtain that the equivalence of the completeness property and parabolicity extends to all flute surfaces whose twists are zero or a half without any assumption on the convexity or size of the length parameters l_n.

Theorem 6.3. *Let* X *be a flute surface whose twists satisfy* $t_n \in \{0, 1/2\}$ *for* $n \geq 1$*. The following are equivalent:*

- *the covering group of X is of the first kind, i.e. X is the union of geodesic pairs of pants without funnels or half-planes,*
- *X does not admit a Green's function, i.e. X is parabolic.*

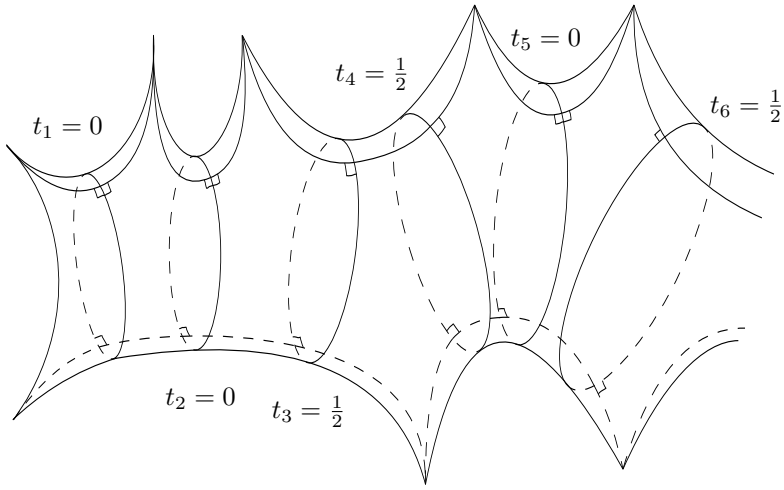

Figure 6.1: The half and zero twists flute surface.

Proof. All that is needed is to prove completeness implies parabolicity. Therefore, assume X is complete. Since the twists are all zero or a half, there exists a collection of bi-infinite geodesics (between cusps) that separate X into two symmetric halves (see Figure 6.1) permuted by an orientation-reversing isometry. In this way, X is symmetric.

Choose one side of X as its front and call it $X^\star$. The front side $X^\star$ is planar and simply connected. Thus, it has a unique isomorphic lift $\tilde{X}^\star$ to the universal cover $\mathbb{D}$ (see Figure 6.2). This lift is an infinite polygon in $\mathbb{D}$, which has countably many vertices on S^1 corresponding to the lifts of the cuffs of X. Consider the geodesic subsurface X_n of X, which is the union of the first n tight pairs of pants. Call the front of the geodesic boundary of X_n the geodesic arc α_n. The lift of α_n in $\tilde{X}^\star$ is called $\tilde{\alpha}_n$. Each $\tilde{\alpha}_n$ connects the top and bottom sides of $\tilde{X}^\star$.

We show that X is complete if and only if, in addition to its countably many vertices on S^1, the top and bottom sides of the infinite polygon $\tilde{X}^\star$ in $\mathbb{D}$ converge to a single point on S^1. If the top and bottom sides converge to two different points on S^1, then the infinite

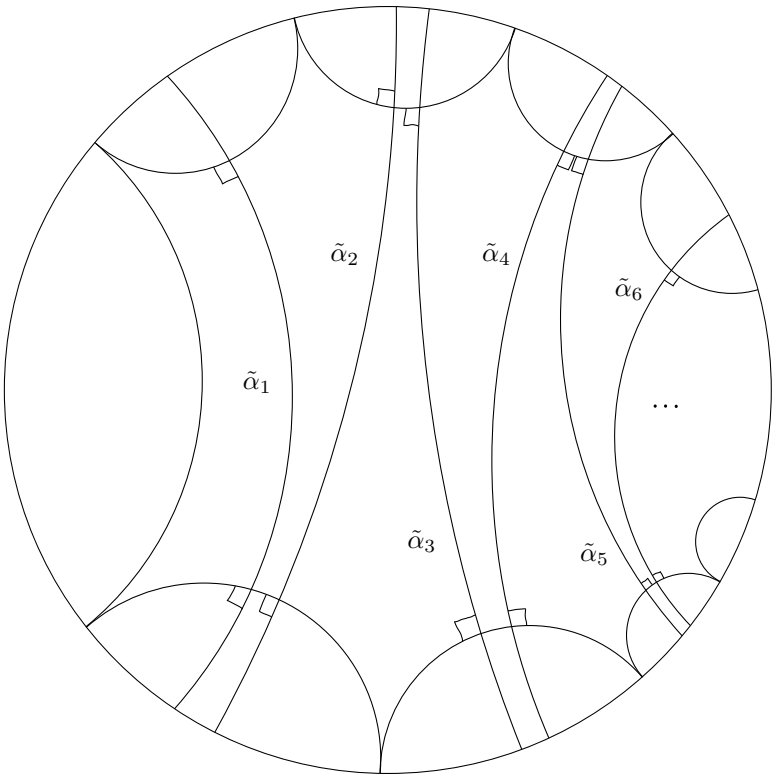

Figure 6.2: Infinite polygon $\tilde{X}^\star$ in $\mathbb{D}$ isometric to $X^\star$.

polygon converges to a single geodesic g_∞ that connects these two points. Thus, X is not complete.

If the top and bottom sides of the infinite polygon converge to a single point on S^1, we show that X is complete. Assume to reach a contradiction that there is a finite length escaping geodesic ray r starting from a point on the boundary of X_1. Reflect each maximal subcurve of r in $X^{\star\star}$ to the front $X^\star$ and call the reflection $r^\star$. Since $r^\star$ is finite length, it is compact. Also, the fact that $r^\star$ is escaping means it intersects every lift $\tilde{\alpha}_n$ in the polygon $\tilde{X}^\star$. The fact that $r^\star$ is both compact and intersects every lift $\tilde{\alpha}_n$ means that the geodesic arcs $\tilde{\alpha}_n$ converge to the geodesic $g^\star$ in $\mathbb{D}$. The endpoints of $\tilde{\alpha}_n$ accumulate to the endpoints of $g^\star$ on S^1. These distinct endpoints of $g^\star$ are the accumulations of the top and bottom sides of the infinite polygon. This contradiction implies X is complete.

What is left to prove is that if the top and bottom sides of the infinite polygon converges to a single point, then X is parabolic. Consider the curve family Γ_n that connects the

boundary of X_1 with the boundary of X_n in $X^\star$ for each n and lift each of them to the infinite polygon in $\mathbb{D}$. Call the lifts of Γ_n, the families of curves $\Gamma_n^\star$ in $\mathbb{D}$. Choose a circle C_R of fixed radius $R > 0$ whose center is the point on S^1 called p that the infinite polygon converges to, and is to the right of $\tilde{\alpha}_1$ in Figure 6.2. Consider large n such that $\tilde{\alpha}_n$ is entirely inside C_R. For each such large n, define C_n to be the circle centered at p of the smallest radius r_n such that C_n contains $\tilde{\alpha}_n$. Define $\Gamma_n'^\star$ to be the family of sub curves of curves in $\Gamma_n^\star$ that connects C_n with C_R for large n.

Let Γ_n^C be the family of curves that connect C_n and C_R for large n. Call A the annulus between circles C_n and C_R for any fixed value of n. Let ρ be a metric on the annulus A. Define $L(\Gamma, \rho) = \inf_\gamma \ell_\rho(\gamma)$ where the infimum is over all curves γ in Γ. In addition, define $A(A, \rho) = \iint_A \rho^2(z)dxdy$. By the Cauchy-Schwartz inequality,

$$L^2(\Gamma_n^C, \rho) \leq (\int_{r_n}^R \rho(te^{i\theta})dt)^2 \leq log(\frac{R}{r_n}) \int_{r_n}^R \rho(te^{i\theta})^2 tdt.$$

Next, integrate both sides with respect to θ from 0 to 2π to get

$$2\pi L^2(\Gamma_n^C, \rho) \leq log(\frac{R}{r_n}) A(A, \rho).$$

Since

$$\text{mod}\Gamma = \inf\{A(\Omega, \rho) : L(\Gamma, \rho) = 1\},$$

we have

$$\text{mod}\Gamma_n^C \geq \frac{2\pi}{log(\frac{R}{r_n})}.$$

Equality holds when applying the Cauchy-Schwartz inequality if and only if $\rho = \frac{c}{|z|}$ almost everywhere for any positive constant c. Thus,

$$\text{mod}\Gamma_n^C = \frac{2\pi}{log(\frac{R}{r_n})}.$$

We get

$$\mathrm{mod}\Gamma_n^\star \leq \mathrm{mod}\Gamma_n'^\star \leq \mathrm{mod}\Gamma_n^C = \frac{2\pi}{log(\frac{R}{r_n})}$$

by first applying the overflowing property of modulus and then the monotonicity property. The top and bottom sides of the infinite polygon in $\mathbb{D}$ converges to a single point on S^1, and the $\tilde{\alpha}_n$ connect points on these top and bottom sides. Thus, the $\tilde{\alpha}_n$ converges to a single point. Consequently, the sequence of radii r_n converges to zero as $n \to \infty$. Thus,

$$lim_{n\to\infty}\mathrm{mod}\Gamma_n^\star = 0.$$

By the modular test and Theorem 5.2, X is parabolic. □

As a direct consequence of the proof of Theorem 6.3, we have the following Corollary.

Corollary 6.4. *A symmetric flute surface X has covering group of the first kind if and only if, in addition to its ideal vertices, the infinite ideal polygon in $\mathbb{D}$ that is a lift of the front side of X accumulates to a single point on S^1.*

6.3 Symmetric surfaces with finitely many ends

For an infinite Riemann surface X, fix a compact exhaustion X_n of X by geodesic subsurfaces. A *topological end* of X is defined to be a decreasing sequence of sets C_n such that C_n is a connected component of $X - X_n$. We say such an end is accumulated by genus if each C_n corresponding to the end has positive genus. Fix a finite genus surface X_0 with finitely many geodesic boundaries $\{\delta_1, ..., \delta_k\}$. Attach to each closed geodesic δ_i a surface X_i with one geodesic boundary and infinite genus that accumulates to one topological end. This construction gives a *symmetric end surface* X (see Figure 6.3). The geodesic surfaces attached to each δ_i can be thought of as *tails of infinite Loch-Ness monsters* (see Figure 6.4).

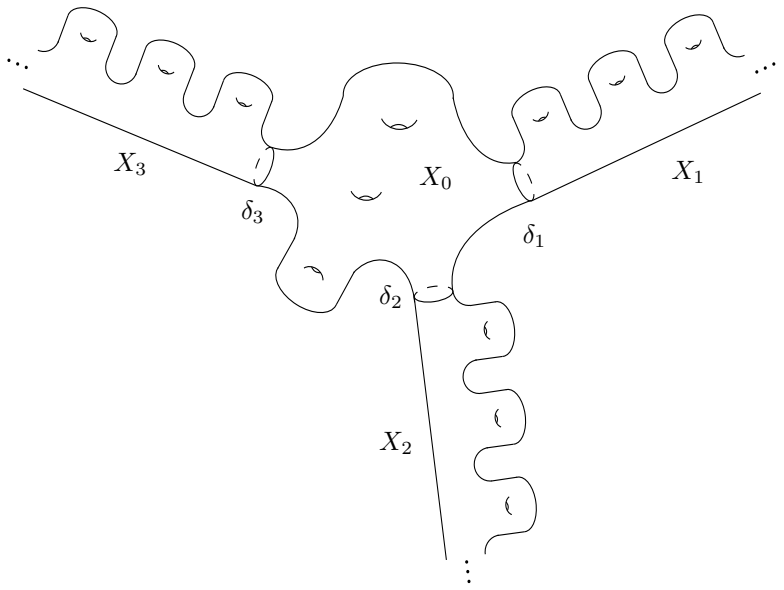

Figure 6.3: A surface with finitely many non-planar ends.

Separate the handles in each attached surface by closed geodesics called β_n. There is a geodesic arc orthogonal to β_n at both of its endpoints. Choose a geodesic loop γ_n orthogonal to this geodesic arc in each handle. Each attached geodesic surface minus the attached handles is an infinite chain of geodesic pairs of pants. Other than the geodesics β_n and γ_n, name the other geodesic boundaries of each end in order by the sequence $\{\alpha_n\}$.

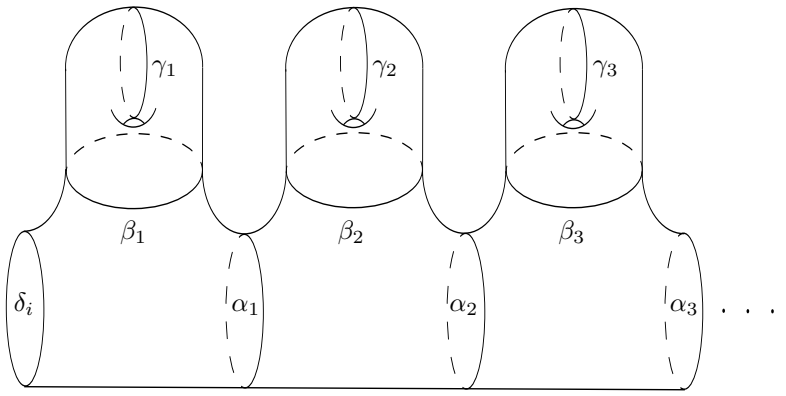

Figure 6.4: The pants decomposition of an end surface.

The set of simple closed geodesics $\{\delta_i, \alpha_n, \beta_n, \gamma_n\}$ separate the surface X into geodesic pairs of pants (see Figure 6.4). Use the unique orthogeodesic arcs between the δ_i, α_n, β_n, and γ_n to separate the geodesic pairs of pants in the decomposition of X into right-angled

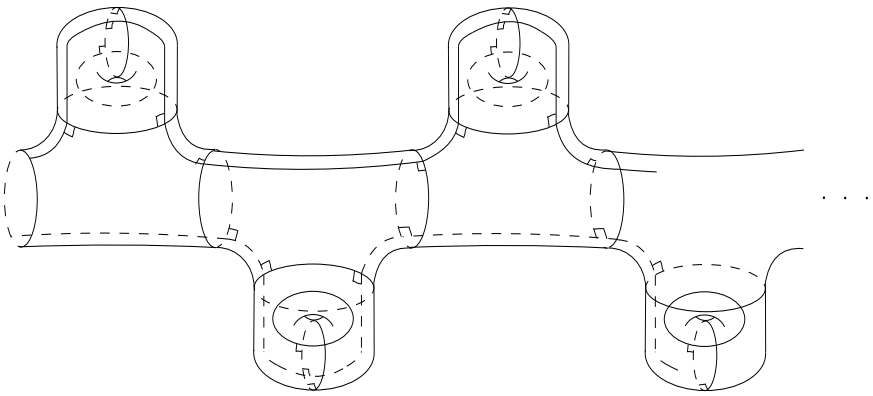

Figure 6.5: A symmetric end surface with half twists.

geodesic hexagons.

A collection of bi-infinite geodesics separates surface X into two symmetric halves. Call one of these halves its front side and denote it by $X^\star$. The other half is called its back side $X^{\star\star}$.

When an attached end X_i of X has a separation into two symmetric halves, the end X_i is called a *symmetric end* (see Figure 6.5). If every end of X is symmetric, then X is a *symmetric end surface* (see Figure 6.3).

Theorem 6.5. *Let X be a Riemann surface with finitely many symmetric non-planar ends such that the lengths of the geodesics β_n and γ_n from Figure 6.3 are between two positive constants. Then the following are equivalent:*

- *the Fuchsian covering group of X is of the first kind,*
- *the Riemann surface X admits no Green's function.*

Remark 6.6. Note that the α_n are not assumed to be bounded. If any subsequence of α_n is bounded, by Theorem 6.1 proved by Basmajian, Hakobyan, and Šarić ([7]), regardless of the twists, X is parabolic. Therefore, the interesting case is when the lengths of α_n go to infinity.

Proof of Theorem 6.5. The problem is simplified to prove that completeness implies parabolicity for X. Separate each X_i into two halves by bi-infinite geodesics and conclude each X_i

is symmetric. Call one half the front side $X_i^\star$ and the other half the back side $X_i^{\star\star}$. The front side $X_i^\star$ is planar but not simply connected due to its infinitely many handles.

We define a compact exhaustion of X by compact subsurfaces X_n of X such that their boundary components are the geodesics α_n in each X_i for $i = 1, \ldots, k$. Let Γ^n be the family of curves that connect the boundary of X_0 and the boundary of X_n in $X_n - X_0$. By the modular test, we only need that $\lim_{n\to\infty} \mathrm{mod}\Gamma_n = 0$. Define $\mathrm{mod}\Gamma_i^n$ to be the subfamily of Γ^n that lies in the end X_i. The sequence of curve families Γ^n is a disjoint union of the Γ_i^n for $i = 1, \ldots, k$. Therefore,

$$\mathrm{mod}\Gamma^n = \sum_{i=1}^{k} \mathrm{mod}\Gamma_i^n.$$

We only need to prove that $lim_{n\to\infty}\mathrm{mod}\Gamma_i^n = 0$ for each $i = 1, \ldots, k$.

The modulus is a quasiconformal quasi-invariant. Thus, $\mathrm{mod}\Gamma_i^n$ tends to zero on X_i if and only if it tends to zero on a quasiconformal image of X_i. The assumption that the lengths of β_n and γ_n are bounded between two positive constants implies that there is a quasiconformal map onto an infinite surface such that the β_n and γ_n are all the same length, and the twists on these closed geodesics are all equal to zero (see Shiga [19]). Without loss of generality, we can assume all of the tori cut off by the β_n in X_i is isometric.

The front of the surface $X_i^\star$ is not simply connected (see Figure 6.6). Notice, however, that $X_i^\star - \cup_n \gamma_n$ is planar, simply connected, and has a unique isomorphic lift to $\mathbb{D}$, as in Figure 6.6. Let $X_i^n = X^n \cap X_i$ and $X_i^{n\star} = X_i^n \cap X_i^\star$ be the front side of X_i^n. Let $\Gamma_i^{n\star}$ be the subfamily of Γ_i^n that lies entirely in the front of X_i^n. By Theorem 4.2 it is enough to prove

$$\lim_{n\to\infty} \mathrm{mod}\Gamma_i^{n^\star} = 0$$

for all $i = 1, \ldots, k$.

Since X has a covering group of the first kind, a single component of the lift to the universal covering $\mathbb{D}$ of $X_i^* \setminus (\cup_n \gamma_n)$ accumulates to exactly one point on S^1. Consequently, the sequence of moduli of the family of curves from $\delta_i \cap X_i^\star$ to α_n in $X_i^\star$ converge to zero as n approaches infinity (in the same way as in the proof of Theorem 6.3).

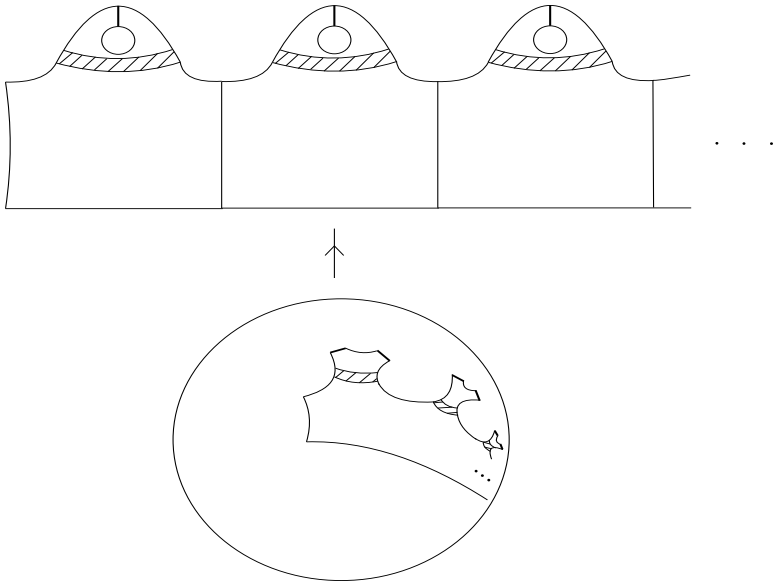

Figure 6.6: The front side $X_i^\star$ and its lift to the universal covering.

However, the above argument does not work for the curves in $X_i^\star$ that intersect the $\{\gamma_n\}_n$. We will find a quasiconformal map that sends $X_i^\star$ into but not onto the lift of $X_i^\star \setminus (\cup_n \gamma_n)$. Then the limit of the modulus of a sequence is zero for the sequence of curve families connecting $\delta_i \cap X_i^\star$ and $\alpha_n \cap X_i^{n\star}$ inside $X_i^{n\star}$. With this the proof is done because a quasiconformal map quasi-preserves the modulus and we already established that the limit of the modulus of the sequence of curve families in $X_i^\star \setminus (\cup_n \gamma_n)$ is zero.

To find the quasiconformal map, observe the standard half-collars around the β_n inside the torus cut off by β_n. These standard collars are disjoint from γ_n. Define X_i' to be $X_i^\star$ minus the tori cut off by the β_n union the standard half collars about the β_n in the cut-off tori. We find a quasiconformal map f that sends $X_i^\star$ into, but not onto X_i'. This quasiconformal map f is also the identity on $X_i^\star$ minus the cut-off tori and the identity on the $\beta_n \cap X_i^\star$. All that remains is to find a quasiconformal map whose image on the front half of the tori cut off by β_n is the front half of the half collar that is the identity on $\beta_n \cap X_i^\star$. We only need one quasiconformal map and use it for all n since the tori are quasiconformal.

Let T_n be the front of a torus cut off by β_n. It is a doubly connected region, and thus we can find a conformal map that maps T_n to a Euclidean annulus with inner radius one

and outer radius $r > 1$. The geodesic subarc of β_n in T_n maps to a curve b_n on the outer circle of the Euclidean annulus. Meanwhile, the boundary of the standard half-collar in the interior of T_n maps to a curve c_n in the interior of the Euclidean annulus. The endpoints of the curve c_n are on the outer circle of the Euclidean annulus minus b_n. Map the Euclidean annulus by a conformal map to the square of height one such that the bottom side is on the real axis and the endpoints of c_n get sent to the top corners of the square. Call the images under this map of b_n and c_n by the same names. This curve c_n has a lowest point of height h. Define the last map, g, by the function that vertically shrinks this square by a factor of h. Conjugate the function g by the composition of the conformal maps. The image of T_n under this conjugation is in the front of the standard half-collar around β_n. Therefore, the conjugation is the desired quasiconformal map f.

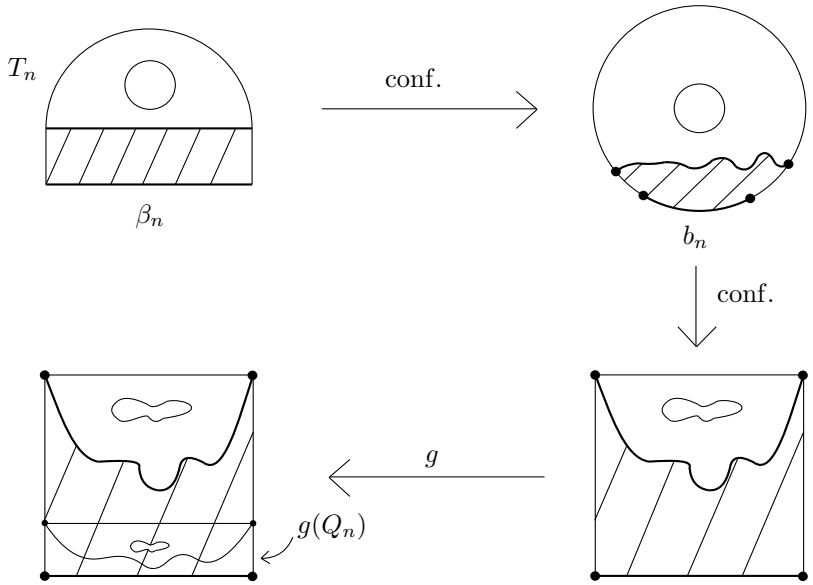

Figure 6.7: The quasiconformal map.

□

The proof of Theorem 6.5 gives the following Corollary.

Corollary 6.7. *A symmetric surface X with finitely many end surfaces X_i, for $i = 1, 2, \ldots n$, has covering group of the first kind if and only if, for each $i \in \{1, 2, \ldots, n\}$, the infinite*

polygon in $\mathbb{D}$ that is a lift of $X_i^* \setminus (\cup_n \gamma_n) \subset X$ accumulates to a single point on S^1.

Remark 6.8. For a fixed lift of $X_i^* \setminus (\cup_n \gamma_n)$ in $\mathbb{D}$, let $\widetilde{\alpha_n}$ be the lift of the closed geodesic α_n that connects its two boundary sides. Then the accumulation to one point of S^1 in the above corollary is equivalent to the accumulation of the nested sequence $\widetilde{\alpha_n}$ to one point of S^1.

Chapter 7

Characterization of parabolicity of symmetric surfaces using their length parameters

In this section, we determine whether or not Riemann surfaces are parabolic using their Fenchel-Nielsen parameters.

7.1 The half-twist flute surfaces

Consider the tight flute surfaces $X = \{(\ell_n, 1/2)\}_n$ with only half twists called half-twist flute surfaces. We characterize the parabolicity of these surfaces using their lengths ℓ_n.

Theorem 7.1. *Let $X = \{(\ell_n, 1/2)\}_n$ be a half-twist flute surface with increasing sequence of cuff lengths ℓ_n. Then X is parabolic if and only if*

$$\sum_{n=1}^{\infty} e^{-\sigma_n/2} = \infty,$$

where $\sigma_n = \ell_n - \ell_{n-1} + \cdots + (-1)^{n-1}\ell_1$.

To prove Theorem 7.1, we need to define what a shear is. Let Δ_1 and Δ_2 be two ideal geodesic triangles with disjoint interiors that share a geodesic g as a side. Orient the geodesic

g so that the ideal triangle Δ_1 is on its left side. The *shear* $s(g)$ of the geodesic g with respect to the configuration (Δ_1, Δ_2) is the signed hyperbolic distance (using the orientation of g) from the foot of the orthogeodesic from the vertex in Δ_1, not on g, to the foot of the orthogeodesic from the vertex in Δ_2 not on g.

Remember, the front $X^\star$ of a half-twist flute surface is planar and simply connected. Thus, its lift $\tilde{X}^\star$ to the universal covering $\mathbb{D}$ is an infinite polygon, as shown in Figure 6.2. Corollary 6.4 gave the covering group of a half-twist flute is of the first kind if and only if, in addition to its countable set of vertices, the infinite polygon $X^\star$ has only one more point of accumulation on S^1.

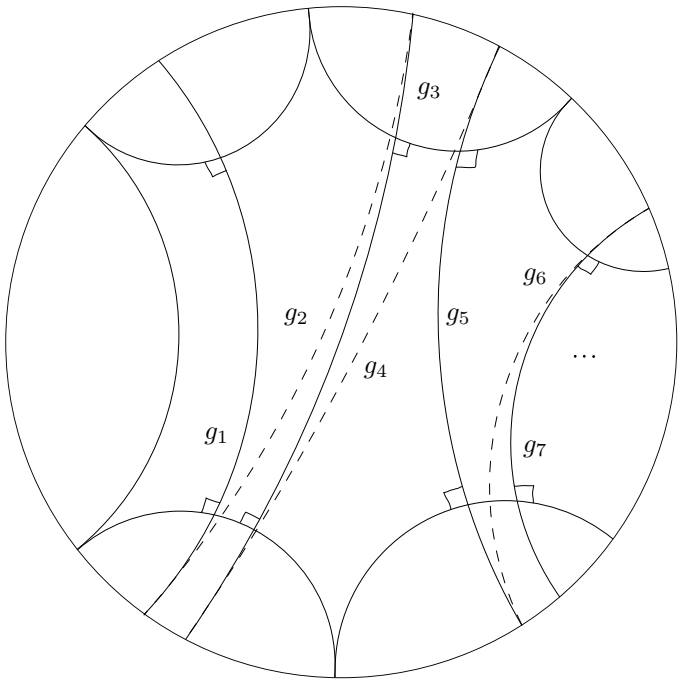

Figure 7.1: The infinite polygon $\tilde{X}^*$ and its limit points on S^1.

Therefore, the only thing we need to prove is, given X has a covering group of the first kind, that the infinite polygon $X^\star$ accumulates to one point on S^1 in addition to its ideal vertices. The fronts of the geodesic boundaries α_n of X lift to the curves $\tilde{\alpha}_n$ in the universal cover $\mathbb{D}$. These lifts $\tilde{\alpha}_n$ lay on corresponding geodesics we call g_{2n-1} (see Figure 7.1). Define the geodesics g_{2n} to connect the initial point of g_{2n-1} and the terminal point of g_{2n+1}. The

result is a nested sequence of geodesics g_n. We want to find the shears $s(g_n)$ for $n \geq 2$ of the geodesics g_n, which are the diagonals of ideal quadrilaterals whose vertices are the endpoints of g_{n-1} and g_{n+1}.

The unique orthogeodesic arc η_n between g_{2n-1} and g_{2n+1} is on the lift of the front side $\tilde{X}^\star$ (see Figure 7.1). The η_n, $\tilde{\alpha}_{2n-1}$, and $\tilde{\alpha}_{2n+1}$ make up three sides of a geodesic pentagon in $\tilde{X}^\star$ with four right angles and one zero angle. The orthogeodesic rays from the vertices of these pentagons with zero angles to the η_n separate each pentagon into two Lambert quadrilaterals. For each such pentagon, the sides on g_{2n-1} and g_{2n+1} have lengths $\frac{\ell_n}{2}$ and $\frac{\ell_{n+1}}{2}$. A formula for Lambert quadrilaterals [11, Theorem 2.3.1(iv)] gives

$$\ell(\eta_n) = \tanh^{-1}\Big(\frac{1}{\cosh\frac{\ell_n}{2}}\Big) + \tanh^{-1}\Big(\frac{1}{\cosh\frac{\ell_{n+1}}{2}}\Big).$$

Using the length $\ell(\eta_n)$ we just obtained, and the inequalities $x < \tanh^{-1}(x) < 2x$ for small $x > 0$, we get

$$e^{-\frac{\ell_{n+1}}{2}} < \frac{1}{\cosh\left(\frac{\ell_n}{2}\right)} + \frac{1}{\cosh\left(\frac{\ell_{n+1}}{2}\right)} < \ell(\eta_n) < \frac{2}{\cosh\left(\frac{\ell_n}{2}\right)} + \frac{2}{\cosh\left(\frac{\ell_{n+1}}{2}\right)} < 8e^{-\frac{\ell_n}{2}}$$

for large n. Therefore, for large n,

$$e^{-\frac{\ell_{n+1}}{2}} < \ell(\eta_n) < 8e^{-\frac{\ell_n}{2}}. \tag{7.1}$$

Lemma 7.2. *Under the above notation, the shear along g_{2n} for the quadrilateral whose vertices are at the endpoints of g_{2n-1} and g_{2n+1} is given by*

$$s(g_{2n}) = \log \sinh^2 \frac{\ell(\eta_n)}{2}.$$

Remark 7.3. Note that $s(g_{2n}) < 0$ for n large enough because $\ell(\eta_n) \to 0$ as $n \to \infty$.

Proof. The hyperbolic distance between g_{2n-1} and g_{2n+1} is $\ell(\eta_n)$. Let $A : \mathbb{D} \to \mathbb{H}$ be a Mobius function that maps η_n to the y-axis. The endpoints of geodesics $A(g_{2n-1})$ and $A(g_{2n+1})$ are

$\{-x_n, x_n\}$ and $\{-y_n, y_n\}$. We can assume without loss of generality that $x_n < y_n$. Then

$$l(\eta_n) = \log \frac{y_n}{x_n}.$$

Define the Mobius function $B : \mathbb{H} \to \mathbb{H}$ by $B(x_n) = 0$, $B(-x_n) = -1$, and $B(-y_n) = \infty$. Then $B(z) = \frac{y_n - x_n}{2x_n} \frac{z - x_n}{z + y_n}$. That implies $B(y_n) > 0$ and

$$s(g_{2n}) = \log(B(y_n)) = \log \left[\frac{y_n - x_n}{2\sqrt{x_n}\sqrt{y_n}} \right]^2 = \log \sinh^2 \frac{\ell(\eta_n)}{2}.$$

□

The remaining cases are to find the shears $s(g_n)$ for geodesics g_n such that n is odd. The expression is trickier to attain as it depends on the lengths of two adjacent η_i and the length of the cuff that lifts to g_n. The formula will be slightly different for indices with remainders 1 and 3 under division by 4.

Lemma 7.4. *Consider the lift of $X^\star$ and geodesics g_n as above. The shear of g_n is defined with respect to the quadrilateral whose vertices are the ideal endpoints of g_{n-1} and g_{n+1}. When ℓ_n is large enough, we have*

$$s(g_{4n+1}) = \sinh^{-1} \frac{1}{\sinh \ell(\eta_{2n})} + \sinh^{-1} \frac{1}{\sinh \ell(\eta_{2n+1})} - \frac{\ell_{2n+1}}{2}$$

and

$$s(g_{4n+3}) = \sinh^{-1} \frac{1}{\sinh \ell(\eta_{2n+1})} + \sinh^{-1} \frac{1}{\sinh \ell(\eta_{2n+2})} + \frac{\ell_{2n+2}}{2}.$$

Proof. Consider g_{4n+1} and the corresponding quadrilateral as in Figure 7.2. Geodesic g_{4n+1} is it's diagonal. Name the vertices of the quadrilateral to the left and right of g_{4n+1}, points A and D, respectively. Then A is the initial point of geodesic g_{4n-1}, and D is the terminal point of g_{4n+3}. Call P the foot of the orthogedoesic from point A to the geodesic g_{4n+1} and S the foot of the orthogeodesic from point D to g_{4n+1}. Let $B \in g_{4n-1}$ and $Q \in g_{4n+1}$ be the endpoints of orthogeodesic η_{2n}. Call $R \in g_{4n+1}$ and $C \in g_{4n+3}$ the endpoints of η_{2n+1} (see Figure 7.2).

The starting choice of the half-twists and because the index of g_i has remainder 1 under division by 4 guarantees that the arc PS is contained in arc RQ (see Figures 7.1 and 7.2). From Figure 7.2 we get

$$s(g_{4n+1}) = \ell(PQ) + \ell(RS) - \frac{\ell_{2n+1}}{2},$$

where $\ell(PQ)$ and $\ell(RS)$ are the hyperbolic lengths of geodesic arcs PQ and RS, respectively. By [11, Theorem 2.3.1(i)], the Lambert quadrilaterals $ABQP$ and $RSDC$ give $\ell(PQ) = \sinh^{-1}\frac{1}{\sinh \ell(\eta_{2n})}$ and $\ell(RS) = \sinh^{-1}\frac{1}{\sinh \ell(\eta_{2n+1})}$. From these lengths we obtain the formula for $s(g_{4n+1})$.

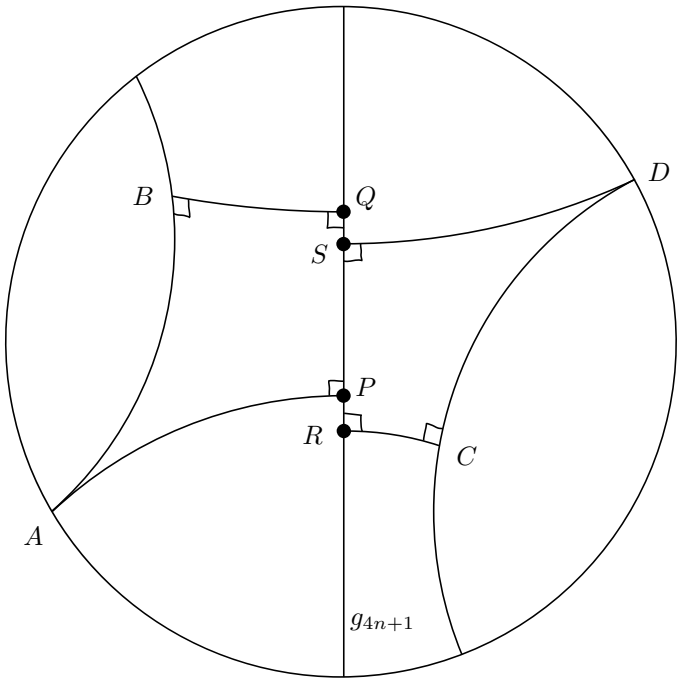

Figure 7.2: $s(g_{4n+1}) = \ell(PQ) + \ell(RS) - \frac{\ell_{2n+1}}{2}$.

Consider g_{4n+3} and the corresponding quadrilateral in Figure 7.3. The geodesic g_{4n+3} is the diagonal of this quadrilateral. Call the vertices of the quadrilateral not on geodesic g_{4n+3}, points A and D to the left and right, respectively. Let P be the foot of the orthogeodesic from point A to geodesic g_{4n+3}, and let S be the foot of the orthogeodesic from point D to the same geodesic. Call B and Q the endpoints of the orthogeodesic η_{2n+1} from g_{4n+1} to g_{4n+3}. Denote the endpoints of the orthogeodesic η_{2n+2} from g_{4n+3} to g_{4n+5} by R and C (see

Figure 7.3).

The starting choice of the half-twists and because the index of g_i has remainder 3 under division by 4 guarantees that the arc QR is contained in arc PS (see Figures 7.1 and 7.3). From Figure 7.3 we obtain

$$s(g_{4n+3}) = \ell(PQ) + \ell(RS) + \frac{1}{2}\ell_{2n+2},$$

where $\ell(PQ)$ and $\ell(RS)$ are the hyperbolic lengths of geodesic arcs PQ and RS, respectively. By [11, Theorem 2.3.1(i)], the Lambert quadrilaterals $ABQP$ and $RSDC$ give $\ell(PQ) = \sinh^{-1}\frac{1}{\sinh \ell(\eta_{2n+1})}$ and $\ell(RS) = \sinh^{-1}\frac{1}{\sinh \ell(\eta_{2n+2})}$. From these lengths, we get the formula for $s(g_{4n+3})$.

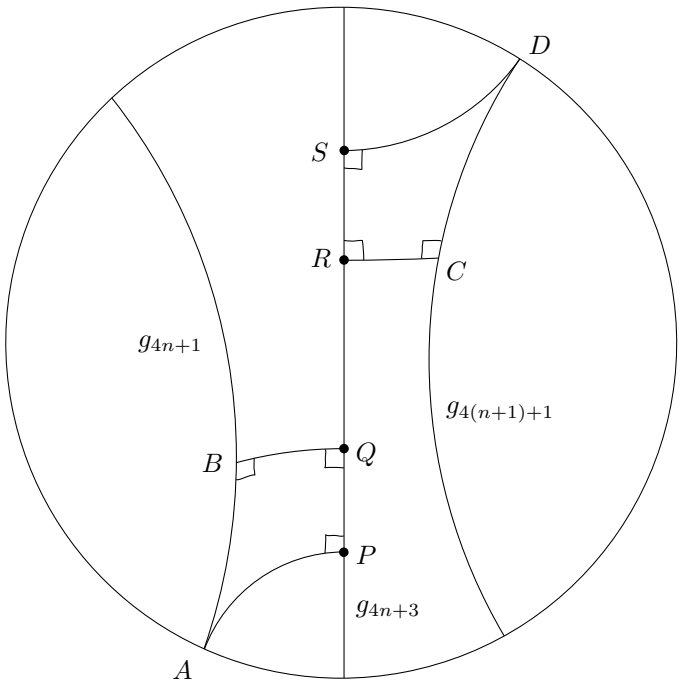

Figure 7.3: $s(g_{4n+3}) = \ell(PQ) + \frac{\ell_{2n+2}}{2} + \ell(RS)$.

□

Proof of Theorem 7.1. By Theorem 6.3, all that is needed is to prove that $X = \{(\ell_n, 1/2)\}_n$ is complete. Due to the symmetry of X, which exchanges its front and back sides, we only

need to prove that the infinite polygon lift of $X^\star$ to $\mathbb{D}$ has only one accumulation point on S^1 in addition to its ideal vertices (see Corollary 6.4). Therefore, it will be enough to prove that the sequence of nested geodesics $\{g_n\}_{n=1}^\infty$ (from Figure 7.1) does not accumulate in $\mathbb{D}$.

Consider an escaping geodesic ray r starting from any fixed point on α_1. Reflect it to the front side of X and call its reflection $r^\star$. The length of the part of $r^\star$ from the front of α_n to the front of α_{n+1} is at least the length $l(\eta_n)$ of the orthogeodesic arc η_n between them. It is immediate that $\sum_{n=1}^\infty \ell(\eta_n) = \infty$ implies that $r^\star$ is infinite length and completeness of X follows. Therefore, we assume that $\sum_{n=1}^\infty \ell(\eta_n) < \infty$ in the rest of the proof.

Observe

$$\ell(\eta_n) > \ln(1 + \ell(\eta_n))$$

for $n \geq 1$. This implies

$$\sum_{n=1}^{\infty} \ln(1 + \ell(\eta_n)) < \infty,$$

which immediately gives

$$1 \leq \prod_{n=1}^{\infty} (1 + \ell(\eta_n)) < \infty. \tag{7.2}$$

By Proposition A.1 in the Appendix (or by the proof of [17, Theorem C]), the sequence $\{g_n\}_{n=1}^\infty$ does not accumulate in $\mathbb{D}$ if and only if the piecewise horocyclic arc connecting the adjacent geodesics has infinite length. Denote by $s_n = s(g_n)$ the shear of g_n with respect to the ideal quadrilateral whose vertices are the ideal endpoints of g_{n-1} and g_{n+1} for $n \geq 2$. The shear of g_1 is not defined. We start the piecewise horocyclic path on g_1 such that the part in the *wedge* between g_1 and g_2 has length e^{-s_1}. By Proposition A.3, the length of the part of the piecewise horocyclic path between g_n and g_{n+1} is

$$e^{-s_1 - s_2 - \cdots - s_n}$$

when n is odd, and it equals

$$e^{s_1 + s_2 + \cdots + s_n}$$

when n is even.

We will use the inequalities

$$e^{\sinh^{-1}\frac{1}{\sinh x}} > \frac{2}{x}$$

and

$$\sinh x > x$$

for $x > 0$.

By Lemmas 7.4 and 7.2 and the above inequalities, we get, for $n \geq 1$,

$$\begin{aligned} e^{s_{4n+1}} &> \tfrac{4}{\ell(\eta_{2n})\ell(\eta_{2n+1})} e^{-\frac{\ell_{2n+1}}{2}}, \\ e^{s_{4n+3}} &> \tfrac{4}{\ell(\eta_{2n+1})\ell(\eta_{2n+2})} e^{\frac{\ell_{2n+2}}{2}}, \text{ and} \\ e^{s_{2n}} &> \tfrac{[\ell(\eta_n)]^2}{4}. \end{aligned} \tag{7.3}$$

Note that the constants 4 are essential for what follows since they will be canceled out which will facilitate the needed inequality comparison.

Since we need a lower estimate of the length of the piecewise horocyclic path, we note that $\ell(h)$ is greater than

$$\sum_{n=1}^{\infty} e^{s_{4n}+s_{4n-1}+\ldots+s_2+s_1}. \tag{7.4}$$

The sum (7.4) can be written as

$$\sum_{n=1}^{\infty}\prod_{k=0}^{n-1} e^{s_{4(k+1)}+s_{4k+3}+s_{4k+2}+s_{4k+1}}$$

and by the estimates in (7.3) we get

$$\begin{aligned} e^{s_{4(k+1)}+s_{4k+3}+s_{4k+2}+s_{4k+1}} &> \frac{[\ell(\eta_{2k+2})]^2}{4} \cdot \frac{4}{\ell(\eta_{2k+1})\ell(\eta_{2k+2})} \cdot e^{\frac{\ell_{2k+2}}{2}} \\ \cdot\frac{[\ell(\eta_{2k+1})]^2}{4} \cdot \frac{4}{\ell(\eta_{2k})\ell(\eta_{2k+1})} \cdot e^{\frac{-\ell_{2k+1}}{2}} &= \frac{\ell(\eta_{2k+2})}{\ell(\eta_{2k})} e^{\frac{\ell_{2k+2}-\ell_{2k+1}}{2}}. \end{aligned} \tag{7.5}$$

This implies

$$\sum_{n=1}^{\infty}\prod_{k=0}^{n-1} e^{s_{4(k+1)}+s_{4k+3}+s_{4k+2}+s_{4k+1}} > C\sum_{n=1}^{\infty}\prod_{k=1}^{n-1}\frac{\ell(\eta_{2k+2})}{\ell(\eta_{2k})}e^{-\frac{\ell_{2k+1}}{2}+\frac{\ell_{2k+2}}{2}}. \tag{7.6}$$

By cancellations we get

$$\prod_{k=1}^{n-1}\frac{\ell(\eta_{2k+2})}{\ell(\eta_{2k})}e^{-\frac{\ell_{2k+1}}{2}+\frac{\ell_{2k+2}}{2}} = \frac{\ell(\eta_{2n})}{\ell(\eta_2)}e^{(\ell_{2n}-\ell_{2n-1}+\cdots+\ell_4-\ell_3)/2}.$$

By (7.1), we have that $\ell(\eta_{2n}) > e^{-\frac{\ell_{2n+1}}{2}}$, which together with (7.6) and the above equality gives for a modified constant C that

$$\sum_{n=1}^{\infty} e^{s_{4n}+s_{4n-1}+\ldots+s_2+s_1} > C\sum_{n=1}^{\infty} e^{-\frac{\sigma_{2n+1}}{2}}. \tag{7.7}$$

By Lemmas 7.4 and 7.2 we obtain

$$\begin{aligned} e^{-s_{4n+1}-s_{4n}-\ldots-s_2} = \big[e^{-\sinh^{-1}\frac{1}{\sinh\ell(\eta_{2n})}}\cdot e^{-\sinh^{-1}\frac{1}{\sinh\ell(\eta_{2n+1})}}\cdot e^{\frac{\ell_{2n+1}}{2}}\big]\cdot \\ \big[\frac{1}{\sinh^2\frac{\ell(\eta_{2n})}{2}}\big]\cdot\big[e^{-\sinh^{-1}\frac{1}{\sinh\ell(\eta_{2n-1})}}\cdot e^{-\sinh^{-1}\frac{1}{\sinh\ell(\eta_{2n})}}\cdot e^{-\frac{\ell_{2n}}{2}}\big]\cdot \\ \big[\frac{1}{\sinh^2\frac{\ell(\eta_{2n-1})}{2}}\big]\cdot\ldots\cdot\big[\frac{1}{\sinh^2\frac{\ell(\eta_1)}{2}}\big] \end{aligned} \tag{7.8}$$

By using the inequalities $e^{-\sinh^{-1}\frac{1}{\sinh x}} > \frac{x}{5}$ and $\frac{e^{-\sinh^{-1}\frac{1}{\sinh x}}}{\sinh\frac{x}{2}} > \frac{1}{1+x}$ for small $x > 0$, we conclude that the right hand side of (7.8) is greater than

$$\big[\prod_{i=1}^{2n}\frac{1}{1+\ell(\eta_i)}\big]^2 e^{-\sinh^{-1}\frac{1}{\sinh\ell(\eta_{2n+1})}}e^{\frac{\ell_{2n+1}-\ell_{2n}+\cdot+\ell_3-\ell_2}{2}}.$$

By the above inequalities and by (7.2) we have for another constant $C > 0$ that

$$\sum_{n=1}^{\infty} e^{-s_{4n+1}-s_{4n}-\ldots-s_2-s_1} > C\sum_{n=1}^{\infty} e^{-\frac{\sigma_{2n+2}}{2}}. \tag{7.9}$$

By summing (7.7) and (7.9) we obtain for some constant $C > 0$ that the piecewise

horocyclic path has length $\ell(h)$ greater than

$$C\sum_{n=1}^{\infty} e^{-\frac{\sigma_n}{2}}$$

and the assumption of the theorem implies that it is of infinite length. Thus $\tilde{X}^*$ accumulates to one point in addition to its vertices. The parabolicity of X follows. □

Here α_n, η_n for $n \geq 1$ are geodesic arcs of lengths $l(\alpha_n)$, $l(\eta_n)$ in $\mathbb{H}$ and lifts of the α_n and η_n in the surface (see Figure 7.4). Let $p_n = \alpha_n \cap \eta_n$ for $n \geq 1$ and $q_n = \eta_{n-1} \cap \alpha_n$ for $n \geq 2$. The α_n, η_n are defined recursively given any α_1 in $\mathbb{H}$ by the following procedure (see right of Figure 7.4). If $\alpha_n = [q_n, p_n]$ is odd, then $\eta_n = [q_{n+1}, p_n]$ is the geodesic arc such that the angle at p_n from α_n to η_n is $\frac{\pi}{2}$. Given $\eta_n = [q_{n+1}, p_n]$ is odd, we define the geodesic arc $\alpha_{n+1} = [p_{n+1}, q_{n+1}]$ such that the angle at q_{n+1} from η_n to α_{n+1} is $\frac{\pi}{2}$. If $\alpha_n = [p_n, q_n]$ is even, $\eta_n = [p_n, q_{n+1}]$ is the geodesic arc such that the angle at p_n from η_n to α_n is $\frac{\pi}{2}$. Given $\eta_n = [p_n, q_{n+1}]$ is even, $\alpha_{n+1} = [q_{n+1}, p_{n+1}]$ is defined such that the angle at q_{n+1} from α_{n+1} to η_n is $\frac{\pi}{2}$. This recursive process is done using python programming on the computer that illustrates the lifts of the closed geodesic arcs α_n and η_n on the half-twist tight flute surface. See Figure 7.5.

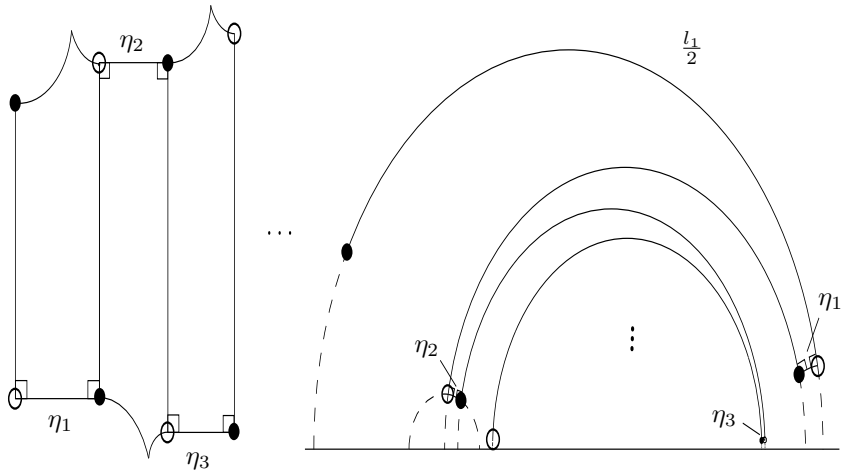

Figure 7.4: Decomposition of one side of the surface into right-angled geodesic pentagons ([BHS], pg 22) and lifts of α_n, η_n.

7.2 The Hakobyan slice of the space of flutes

Let $X_{a,b}$, with $a > 0$ and $b > 0$, and

$$\ell_{2n} = a\ln(n+1) + b\ln n, \quad \ell_{2n+1} = (a+b)\ln(n+1)$$

be a half-twist flute surface with the above lengths of geodesics on the boundary of a pants decomposition (see [7]). Notice that $\{\ell_n\}$ is an increasing sequence because $l_{2n+1} - l_{2n} = bln(\frac{n+1}{n}) > 0$ and $l_{2n} - l_{2n-1} = aln(\frac{n+1}{n}) > 0$ for all n. Basic calculations give $\sigma_{2n+1} = b\ln(n+1) + \ell_1$ and $\sigma_{2n} = a\ln(n+1) - \ell_1$. By Theorem 7.1 we have that $X_{a,b}$ is parabolic if and only if $\sum_{n=1}^{\infty} e^{-\frac{\sigma_n}{2}} = \infty$. The notation $a \asymp b$ means there exist two positive constants K_1 and K_2 such that $K_1 < \frac{a}{b} < K_2$. By computations in [7, Example 9.9], we get that

$$\sum_{n=1}^{\infty} e^{-\frac{\sigma_n}{2}} = \sum_{n\geq 0} e^{-\frac{\sigma_{2n+1}}{2}} + \sum_{n\geq 1} e^{-\frac{\sigma_{2n}}{2}}$$

$$= e^{-\frac{\ell_1}{2}} \sum_{n\geq 0} \frac{1}{(n+1)^{\frac{b}{2}}} + e^{\frac{\ell_1}{2}} \sum_{n\geq 1} \frac{1}{(n+1)^{\frac{a}{2}}} \asymp \sum_{k=1}^{\infty} k^{-\frac{\min(a,b)}{2}}.$$

Conclude that the two domains $X_{a,b} =?$ consist entirely of parabolic flutes in Figure 1.2.

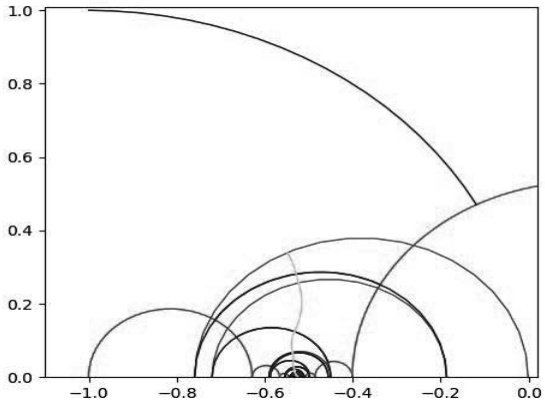

Figure 7.5: A computer generated path of horocyclic concatenations for the flute surface $X_{a,b}$ with $a = 4$ and $b = 1$.

7.3 The symmetric finite ends surfaces

Let X be a Riemann surface with finitely many ends accumulated by genus as defined in Section 6.3. Denote the ends of X by the collection $\{X_i\}_{i=1}^{i=k}$. The handles in any end X_i are cut off by simple closed geodesics β_n. In each handle, choose a simple closed geodesic γ_n. Denote the remaining geodesic boundaries accumulating in each end X_i by α_n and their lengths by l_n. The $\delta_i, \alpha_n, \beta_n$, and γ_n separate the surface X into geodesic pairs of pants, and the unique orthogeodesics between them divide each pants into right-angled geodesic hexagons. When the twists on the α_n in each end X_i of X are all $\frac{1}{2}$, then X is called a *half-twist symmetric ends surface.*

Theorem 7.5. *Let X be a hyperbolic surface with finitely many end surfaces $\{X_i\}_{i=1}^{k}$ accumulated by genus as in Figure 6.3. Assume that the lengths of the simple closed geodesics β_n and γ_n are between two positive constants for each end surface. Let ℓ_n be the lengths of simple closed geodesics α_n accumulating at each end. Assume that ℓ_n is an increasing sequence and the twists on α_n are all equal to $1/2$. Then, for each X_i,*

$$\sum_{n=1}^{\infty} e^{-\frac{\sigma_n}{2}} = \infty$$

if and only if X is parabolic, where $\sigma_n = \ell_n - \ell_{n-1} + \cdots + (-1)^{n-1}\ell_1$.

Proof. Assume $\sum_{n=1}^{\infty} e^{-\frac{\sigma_n}{2}} = \infty$ for any fixed end X_i. Up to a quasiconformal map, we can assume without loss of generality that the cut-off tori are isometric. In other words, we can assume the simple closed geodesics β_n and γ_n have the same length, and their twists are all 0. There exists a front to back decomposition of X. Denote the front side of the end surface X_i by $X_i^\star$. Let $\widetilde{\alpha_n}$ be the lifts of α_n that connect the two boundary sides of a single isomorphic lift of $X^\star \setminus \cup_n \gamma_n$. The $\widetilde{\alpha_n}$ are nested geodesic arcs, and by Remark 6.8, it is enough to prove that the $\widetilde{\alpha_n}$ accumulate to a single point on S^1. We adopt the computation from the proof of Theorem 7.1.

Let g_{2n-1} be the geodesic that contains the lift $\widetilde{\alpha_n}$ for $n = 1, 2, \ldots$ and let g_{2n} be the added geodesic which shares one endpoint with g_{2n-1} and its other endpoint with g_{2n+1} as in Figure

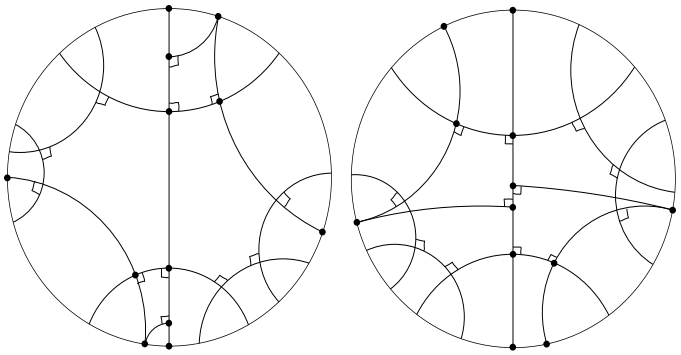

Figure 7.6: Lift of half of pairs of pants of Loch-Ness monster and associated shears.

7.1. Denote the orthogeodesic arc between the geodesics g_{2n-1} and g_{2n+1} by η_n. The lift $X_i^\star$ separates into right-angled hexagons that contain η_n as one of its sides, and whose adjacent sides of length $\frac{\ell_n}{2}$ and $\frac{\ell_{n+1}}{2}$ lie on the geodesics g_{2n-1} and g_{2n+1}. The side opposite η_n in these hexagons is a lift of half of β_n whose length is $\frac{\ell(\beta_n)}{2}$ (see Figure 7.6). Since $\ell_n \to \infty$ as $n \to \infty$ and $\ell(\beta_n)$ is bounded, we can assume without loss of generality that, for some $\ell_0 > 2$, $\ell_n \geq \ell_0 > 2$ and

$$2e^{\frac{\ell(\beta_n)}{2} - \frac{\ell_{n+1}}{2} - \frac{\ell_n}{2}} < 2 \tag{7.10}$$

for $n \geq 1$.

Use the formula for right-angled geodesic hexagons in ([9], Theorem 7.19.2) to get

$$\ell(\eta_n) = \cosh^{-1} \frac{\cosh\left(\frac{\ell(\beta_n)}{2}\right) + \cosh\left(\frac{\ell_{n+1}}{2}\right)\cosh\left(\frac{\ell_n}{2}\right)}{\sinh\left(\frac{\ell_{n+1}}{2}\right)\sinh\left(\frac{\ell_n}{2}\right)}.$$

In order to get a lower estimate for $\ell(\eta_n)$, observe

$$\cosh^{-1}(1+x) > \sqrt{x} \tag{7.11}$$

for $0 < x < 2$. This inequality holds since

$$\begin{aligned} \cosh^{-1}(1+0) &= \sqrt{0} = 0, \\ \frac{d}{dx}(\cosh^{-1}(1+x)) &= \frac{1}{\sqrt{x^2+2x}} > \frac{1}{2\sqrt{x}} = \frac{d}{dx}(\sqrt{x}) \end{aligned}$$

for $0 < x < 2$. The initial assumption (7.10), (7.11), the hexagon formula, and the fact that the ℓ_n are increasing give

$$\begin{aligned}\ell(\eta_n) &> \cosh^{-1}\frac{\frac{1}{2}e^{\frac{\ell(\beta_n)}{2}}+\frac{1}{4}e^{\frac{\ell_{n+1}}{2}+\frac{\ell_n}{2}}}{\frac{1}{4}e^{\frac{\ell_{n+1}}{2}+\frac{\ell_n}{2}}} = \cosh^{-1}\left(1+2e^{\frac{\ell(\beta_n)}{2}-\frac{\ell_{n+1}}{2}-\frac{\ell_n}{2}}\right)\\ &> \sqrt{2}e^{\frac{\ell(\beta_n)-\ell_{n+1}-\ell_n}{4}} > e^{-\frac{\ell_{n+1}}{2}}.\end{aligned}$$

The proof of an upper estimate for $\ell(\eta_n)$ needs the inequality

$$\cosh^{-1}(1+x) < 2\sqrt{x} \tag{7.12}$$

for $x > 0$. The inequality holds because

$$\begin{aligned}\cosh^{-1}(1+0) &= 2\sqrt{0} = 0,\\ \frac{d}{dx}(cosh^{-1}(1+x)) &= \frac{1}{\sqrt{x^2+2x}} < \frac{1}{\sqrt{x}} = \frac{d}{dx}(2\sqrt{x})\end{aligned}$$

for $x > 0$. Then,

$$\frac{\cosh\left(\frac{\ell(\beta_n)}{2}\right)+\cosh\left(\frac{\ell_{n+1}}{2}\right)\cosh\left(\frac{\ell_n}{2}\right)}{sinh(\frac{\ell_{n+1}}{2})sinh(\frac{\ell_n}{2})} < 1+\frac{8e^{\max\{\frac{\ell(\beta_n)}{2}-\frac{\ell_{n+1}}{2}-\frac{\ell_n}{2},-\ell_{n+1},-\ell_n\}}}{1-2e^{-2\ell_0}}.$$

By (7.12),

$$\begin{aligned}l(\eta_n) &< cosh^{-1}(1+\frac{8}{1-2e^{-2\ell_0}}e^{\max\{\frac{\ell(\beta_n)}{2}-\frac{\ell_{n+1}}{2}-\frac{\ell_n}{2},-\ell_{n+1},-\ell_n\}})\\ &< \frac{4\sqrt{2}}{\sqrt{1-2e^{-2\ell_0}}}e^{\max\{\frac{\ell(\beta_n)}{4}-\frac{\ell_{n+1}}{4}-\frac{\ell_n}{4},-\frac{\ell_{n+1}}{2},-\frac{\ell_n}{2}\}}\\ &< \frac{4\sqrt{2}}{\sqrt{1-2e^{-2\ell_0}}}e^{\frac{\ell(\beta_n)}{4}}e^{-\frac{\ell_n}{2}}.\end{aligned}$$

With the bound on $\ell(\beta_n)$, this gives the desired upper estimate.

We have

$$e^{-\frac{\ell_{n+1}}{2}} < \ell(\eta_n) < Ce^{-\frac{\ell_n}{2}}$$

for some $C > 0$ and for $n \geq 1$.

The proof that $\sum_{n=1}^{\infty} e^{s_{4n}+s_{4n-1}+\ldots+s_2+s_1} > C\sum_{n=1}^{\infty} e^{-\frac{\sigma_{2n+1}}{2}}$ follows by the same lines as in the proof of Theorem 7.1 because the geometric positions of the geodesics determining the shears on g_n are identical as seen in Figure 7.6. The above estimate $e^{-\frac{\ell_{n+1}}{2}} < \ell(\eta_n)$ finishes the proof of the inequality.

The proof that $\sum_{n=1}^{\infty} e^{-s_{4n+1}-s_{4n}-\ldots-s_2-s_1} > C\sum_{n=1}^{\infty} e^{-\frac{\sigma_{2n+2}}{2}}$ also follows by the proof of Theorem 7.1 and the geometric positions in Figure 7.6.

Assume $\sum_{n=1}^{\infty} e^{-\frac{\sigma_n}{2}} < \infty$ for some X_i. Similar to the method performed in [7, pgs 41-42] for half-twist flutes, we form a concatenation p of the summits of Saccheri quadrilaterals with bases η_n starting from the point on α_1 furthest from η_1 that escapes the end X_i. Consequently, the length of the n-th summit is at most $Ce^{-\frac{\sigma_{n-1}}{2}}$ for some positive constant C. The path p is finite from our assumption, and the fact that X is not parabolic immediately follows. □

Consider the same symmetric end surface X with finitely many ends accumulated by genus except for each X_i, the twists on the geodesics $\{\alpha_n\}_{n=1}^{\infty}$ accumulating to its end are 0 as in Figure 6.4.

Theorem 7.6. *Let X be a hyperbolic surface with finitely many end surfaces $\{X_i\}_{i=1}^{k}$ accumulated by genus as in Figure 6.2. Assume that the lengths of the simple closed geodesics β_n and γ_n are between two positive constants for each end surface. Let ℓ_n be the lengths of simple closed geodesics α_n accumulating at each end. Assume that ℓ_n is an increasing sequence and the twists on α_n are all equal to 0. Then, for each X_i,*

$$\sum_{n=1}^{\infty} e^{-\frac{l_n}{2}} = \infty$$

if and only if X is parabolic.

Proof. Assume $\sum_{n=1}^{\infty} e^{-\frac{l_n}{2}} = \infty$ in each end X_i. Since $e^{-\frac{l_{n+1}}{2}} < l(\eta_n)$ for all n, we obtain $\sum_{n=1}^{\infty} l(\eta_n) = \infty$. We prove that every escaping geodesic ray in X_i is infinite in length. The parabolicity of X follows by Theorem 6.5.

Denote the front half of the end X_i by $X_i^{\star}$. Consider a geodesic ray r from a point on the

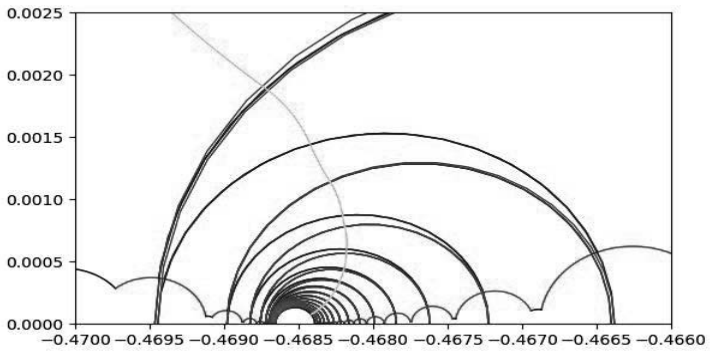

Figure 7.7: A computer-generated path of horocyclic concatenations for the Loch-Ness monster surface $X_{a,b}$ with $a = .5$ and $b = 6.2$.

closed geodesic α_1 in end, X_i, which escapes that end. Reflect r to the front $X_i^\star$. We obtain a piecewise geodesic arc $r^\star$ in $X_i^\star$ with the same length as r.

There are two cases to consider. The first case is that $r^\star$ enters finitely many (including possibly zero) attached toruses in X_i. In such a case, $r^\star$ eventually enters no toruses. Notice that after this point, the length of $r^\star$ between α_n and α_{n+1} is at least the length of η_n. Since $\sum_{n=k}^{\infty} l(\eta_n) = \infty$, the length of $r^\star$ is infinite.

The second case is that $r^\star$ enters infinitely many attached toruses. Since the lengths of β_n and γ_n are between two positive constants, we can assume without loss of generality that the attached toruses are isomorphic. Therefore, the length of every β_n is the same, and each has a zero twist. That means the collar widths around each of the β_n are the same. Since $r^\star$ passes through the full width of infinitely many identical collars, the length of $r^\star$ is infinite.

Assume $\sum_{n=1}^{\infty} e^{-\frac{l_n}{2}} < \infty$. Recall $l(\eta_n) < Ce^{-\frac{l_n}{2}}$ for some $C > 0$ and for $n \geq 1$. That implies the path along the η_n in X is finite. Therefore, the covering group is of the second kind, and X is not parabolic. □

Chapter 8

Non-ergodicity of the geodesic flow on a special class of Cantor tree surfaces

A Riemann surface X is parabolic, denoted by $X \in O_G$, if it does not admit a Green's function-i.e., a harmonic function $u : X \to \mathbb{R}^+$ with a logarithmic singularity at a single point of X whose values limit to zero at the ideal boundary (Ahlfors-Sario [3]). It is known that $X \in O_G$ if and only if the geodesic flow (for the conformal hyperbolic metric) on the unit tangent bundle of X is ergodic if and only if the Poincaré series for the covering Fuchsian group diverges if and only if the Brownian motion on X is recurrent (see Nicholls [15], Sullivan [20], Tsuji [21], Basmajian-Hakobyan-Šarić [7]).

When X is of finite type, then $X \in O_G$ if and only if X has finite area. A Riemann surface X is said to be *infinite* if its fundamental group cannot be finitely generated. An infinite Riemann surface is determined by a fixed geodesic pants decomposition and the Fenchel-Nielsen parameters associated to the pants decomposition (Basmajian-Šarić [8]). As in [7], we consider the question of deciding when $X \in O_G$ based on its Fenchel-Nielsen parameters.

A Cantor tree Riemann surface X_C is conformal to the complement of a Cantor set in the Riemann sphere. Equivalently, X_C is constructed by isometrically gluing countably many geodesic pairs of pants along their boundary geodesics (called *cuffs*) to form the "shape" of the dyadic tree (see Figure 1.3). In addition to the lengths of its cuffs, the Cantor tree

Riemann surface X_C is determined by the twists along the cuffs.

The cuffs of X_C are grouped in the levels based on the level in the dyadic tree. At level zero, we have a single cuff, which is at the top of X_C in Figure 1.3. At level one, we have four cuffs, and at level $n \geq 1$, we have 2^{n+1} cuffs. Denote by $\{\alpha_n^j\}_{j=1}^{2^{n+1}}$ the level n cuffs from left to right in Figure 1.3.

McMullen [13] proved if there is a $C > 0$ such that $1/C \leq \ell(\alpha_n^j) \leq C$ then $X \notin O_G$. This is a consequence of the fact that the Brownian motion has many directions to escape to infinity when the ideal boundary is large, in our case the Cantor set, and the cuffs (the openings) are not short. In the case when the cuffs are short Basmajian, Hakobyan and Šarić [7] proved $X_C \in O_G$ if there is $C > 0$ such that

$$\ell(\alpha_n^j) \leq C\frac{n}{2^n},$$

where $\ell(\cdot)$ is the hyperbolic length in X.

More recently, Šarić [18, Theorem 8.3] proved that if

$$\ell(\alpha_n^j) = \frac{n^r}{2^n}$$

for $r > 2$, and for all $n \geq 1$ and $j = 1, 2, \ldots, 2^{n+1}$ then $X \notin O_G$. Thus, the Brownian motion escapes to infinity even when the cuffs are short in this controlled fashion.

The remaining case to consider is whether X_C is parabolic or not for $1 < r \leq 2$. We show the following.

Theorem 8.1. *Let X_C be the Cantor tree surface as depicted in Figure 1.3 and $\{\alpha_n^j\}_{j=1}^{2^{n+1}}$ the cuffs at the level n. The cuff lengths are decreasing along each end. Then $X_C \notin O_G$ if there is an $r > 1$ such that*

$$C_1\frac{n^r}{2^n} \leq \ell(\alpha_n^j) \leq \frac{C_2}{n^2}$$

for some universal constants $C_1, C_2 > 0$.

Even for $r > 2$, the scope of our theorem is slightly more general than [18, Theorem

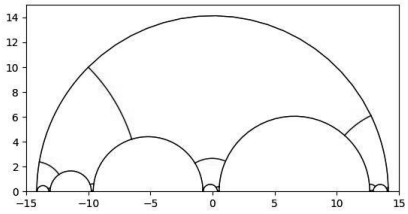

Figure 8.1: A computer-generated picture of an isomorphic lift to $\mathbb{H}$ of the front of a Cantor tree X. Lengths of cuffs vary between bounds in Theorem 8.1, where $r = 1.5$. The picture shows its geodesic flow escapes to infinity along every end due to the sizes of its cuffs. In the picture, X is not parabolic since its Dirichlet integral is finite. There is a large amount of space on X for the geodesics to escape towards many components of its end space $\delta_\infty X$.

8.3] because we allow the lengths of the cuffs to vary with the given lower bound. We also extend our result to surfaces with infinite genus and a Cantor set of ends, called the *blooming Cantor tree surfaces* $\tilde{X}_C$ (see Figure 1.4). To construct the blooming Cantor tree from the Cantor tree, attach a geodesic surface of genus at most C and two boundaries, or do not, to each level n boundary α_n^j (see that $\alpha_0^1 = \alpha_0^2 = \alpha_0$) and redefine α_n^j to be the boundary of the attached surface further away from α_0 for $n \geq 0$ and for $1 \leq j \leq 2^{n+1}$ and for a universal constant $C > 0$. We can add 2^{n+1} surfaces at the level n of genus at most C for $n \geq 0$. Assume the lengths of cuffs along each attached geodesic surface are decreasing.

Theorem 8.2. *Let $\tilde{X}_C$ be the blooming Cantor tree surface and $\{\alpha_n^j\}_{j=1}^{2^{n+1}}$ the cuffs at the level n as depicted in Figure 1.4. The cuff lengths are decreasing along each end and each geodesic subsurface between level n and level $n+1$ boundaries of $\tilde{X}_C$ has genus bounded above by $C > 0$. Then $\tilde{X}_C \notin O_G$ if there is an $r > 1$ such that*

$$C_1 \frac{n^r}{2^n} \leq \ell(\alpha_n^j) \leq \frac{C_2}{n^2}$$

for some universal constants $C_1, C_2 > 0$.

8.1 Partial measured foliations and a sufficient condition for a surface to be non-parabolic

Let $X = \mathbb{H}/\Gamma$ be an infinite Riemann surface, where $\mathbb{H}$ is the hyperbolic plane and Γ is a Fuchsian covering group. For our purposes, a special case of the definition in [18] with $E_i = U_i$ is enough.

Definition 8.3 ([18])**.** A *partial measured foliation* $\mathscr{F}$ on X is an assignment of a collection of sets $\{U_i\}_i$ of X (which do not have to cover the entire surface X) and continuously differentiable (with surjective tangent map) real-valued functions

$$v_i : U_i \to \mathbb{R}.$$

The sets U_i are closed Jordan domains with piecewise differentiable boundaries. We define an arc in X to be the image of a continuous function from a closed interval into X. The pre-image $v_i^{-1}(c)$ for $c \in \mathbb{R}$, if non-empty, is a connected differentiable arc with endpoints on ∂U_i, and

$$v_i = \pm v_j + const \tag{8.1}$$

on $U_i \cap U_j$. The collection of sets $\{U_i\}_i$ is *locally finite* in X.

Let $\mathscr{F}$ be a fixed partial measured foliation on the surface X. An arc in X is said to be a *horizontal arc* if it is expressible as a finite or infinite connected union of arcs defined by $v_i^{-1}(c_i)$ for some collection of real numbers c_i. When an arc in X is a maximal horizontal arc, it is called a *horizontal trajectory* of $\mathscr{F}$. A partial measured foliation is *proper* if each end of the lift to the universal cover $\mathbb{H}$ of every horizontal trajectory approaches a distinct point on the ideal boundary of $\mathbb{H}$.

The *Dirichlet integral* (see [3]) of a continuously differentiable function $v_i : U_i \to \mathbb{R}$ is

$$\int_{U_i} [(\frac{\partial v_i}{\partial x})^2 + (\frac{\partial v_i}{\partial y})^2] dxdy. \tag{8.2}$$

The Dirichlet integral $D_X(\mathscr{F})$ of $\mathscr{F}$ over X is

$$D_X(\mathscr{F}) = \sum_i \int_{U_i} [(\frac{\partial v_i}{\partial x})^2 + (\frac{\partial v_i}{\partial y})^2] dxdy,$$

when the U_i's are non-overlapping sets up to a set of measure zero. A proper partial measured foliation $\mathscr{F}$ on X is *integrable* if $D_X(\mathscr{F}) < \infty$.

From [18, Theorem 3.3] and [18, Theorem 4.1] it immediately follows

Theorem 8.4. *If there is a non-trivial integrable partial measured foliation of a Riemann surface X with leaves that escapes every compact subset of X at both ends, then X is not parabolic.*

8.2 Proof of Theorems 8.1 and 8.2

Define *a to be asymptotic to b*, denoted by $a \asymp b$, to mean that there is a constant $1 \leq k < \infty$ such that $\frac{1}{k} \leq \frac{a}{b} \leq k$. Define *$a$ to be asymptotically less than b*, notated by $a \lesssim b$, to mean that there is a constant $1 \leq k < \infty$ such that $\frac{a}{b} \leq k$.

It is enough to construct an integrable partial measured foliation on X_C when all twists are zero because varying the twists by a bounded amount is a quasiconformal deformation [4] and parabolicity is a quasiconformal invariant [3]. Each geodesic pair of pants is divided into two right-angled hexagons by three orthogeodesic arcs between the pairs of cuffs. Since all twists are zero, the union of the orthogeodesic arcs forms a family of bi-infinite geodesics that separates X_C into two symmetric halves permuted by an orientation-reversing isometry (see Figure 1.3).

Consider a pair of pants Π from the decomposition with boundaries α_1, α_2, and α_3. Let $o_{i,j}$ be the orthogeodesic arc between α_i and α_j, for $i, j \in \{1, 2, 3\}$ such that $i \neq j$. The union $o_{1,2} \cup o_{1,3} \cup o_{2,3}$ separates Π into front and back hexagons H_1 and H_2 with geodesic boundaries. Let a_1 be the orthogeodesic from α_1 to $o_{2,3}$ that separates H_1 into two right-angled pentagons and divides α_1 in H_1 from left to right into the sub-arcs p and q. Call P_p the pentagon containing p (see Figure 8.2), and P_q the pentagon containing q. Since the

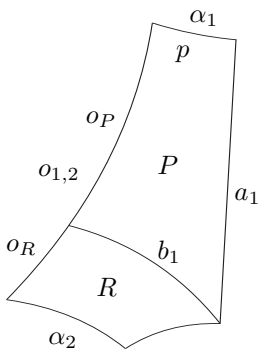

Figure 8.2: Horizontal foliation through $P \cup R$.

lengths of α_2 and α_3 are not necessarily the same, p is not necessarily equal to q.

The orthogeodesic b_1 from $a_1 \cap o_{2,3}$ to $o_{1,2}$ divides P_p into quadrilaterals P and R adjacent to α_1 and α_2. Let o_P be the sub-arc of $o_{1,2}$ in P and let o_R be the sub-arc of $o_{1,2}$ in R (see Figure 8.2). Lift P isometrically to $\mathbb{H}$ as follows. Lift the geodesic arc o_P, starting at α_1, to the y-axis from i to $e^{\ell(o_P)}i$ and call it $\tilde{o}_P$. Each point w in P belongs to a hyperbolic geodesic arc γ_{w_0} orthogonal to o_P with foot w_0 on o_P. Map γ_{w_0} to the geodesic arc $\tilde{\gamma}_{w_0}$ orthogonal to the y-axis in $\mathbb{H}$, to its right, and whose foot on the y-axis is the lift $\tilde{w}_0$ of w_0 for each w_0 in o_P. That defines an isometric lift $\tilde{P}$ of P to $\mathbb{H}$. Denote the lift of a_1 by $\tilde{a}_1$.

Consider the hyperbolic Lambert quadrilateral $ABCD$ such that $\angle CDA$ is acute.

We will use the equations

$$\begin{aligned}
\cosh(BC) &= \tanh(CD)\coth(AB), \\
\sinh(AD) &= \sinh(BC)\cosh(CD), \\
\cos(\angle CDA) &= \sinh(BC)\sinh(AB), \\
\cosh(BC) &= \cosh(AD)\sin(\angle CDA)
\end{aligned}$$

from [11, Theorem 2.3.1(iv), (v), (i), (iii)]. For any right-angled pentagon with consecutive sides a, b, c, d, and e, we will use the equation

$$\cosh(c) = \coth(b)\coth(d)$$

from [11, Theorem 2.3.4(ii)]. Additionally, for any right-angled hexagon with consecutive sides a_1, b_2, a_3, b_1, a_2, and b_3, we will use the equation

$$\cosh(b_1)\sinh(a_2)\sinh(a_3) = \cosh(a_1) + \cosh(a_2)\cosh(a_3) \tag{8.3}$$

from [9, Theorem 7.19.2]. For a pentagon with consecutive side-lengths a, b, c, d, and e such that the angle opposite the side of length b has measure ϕ and the remaining angles are right-angles, we will use the equation

$$\cosh(a)\cosh(c) + \cos(\phi) = \sinh(a)\cosh(b)\sinh(c)$$

from [9, Theorem 7.18.1].

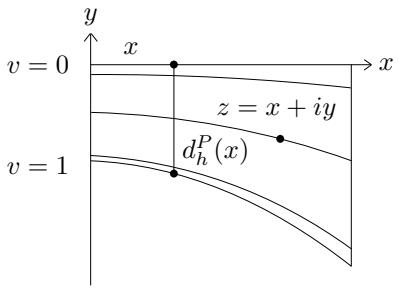

Figure 8.3: The image $f(\tilde{P})$ of a lift of Lambert quadrilateral P in X by a diffeomorphism f.

Map $\tilde{o}_P$ to $[0, \ell(o_P)]$ on $\mathbb{R}$ and each $\tilde{\gamma}_{w_0}$ in $\mathbb{H}$ to a Euclidean segment orthogonal to $[0, \ell(o_P)]$ that is below the x-axis and has Euclidean length equal to its hyperbolic length in $\mathbb{H}$. That defines $f : \tilde{P} \to \mathbb{C}$ (see Figure 8.3). The Euclidean length of $f(\tilde{\gamma}_{w_0})$, where $f(\tilde{w}_0) = x$, by the definition of f and a formula for Lambert quadrilaterals from [11, Theorem 2.3.1(iv)] is

$$d_h^P(x) = \tanh^{-1}(\cosh x \tanh \ell(p)). \tag{8.4}$$

Define a real-valued, continuously differentiable function v_P with $d_h^P(x)$ from (8.4) to be

$$v_P(x + iy) = \frac{y}{-d_h^P(x)} = \frac{-y}{\tanh^{-1}(\cosh x \tanh \ell(p))}$$

for $z = x + iy$ in $f(\tilde{P})$. The function $v = v_P$ defines a horizontal foliation in $f(\tilde{P})$ with

leaves defined by $v_P^{-1}(c)$ for $0 \leq c \leq 1$ (see Figure 8.3). We obtain an upper estimate of the integrand of the Dirichlet integral over $f(\tilde{P})$ and then use it to estimate the integral for sufficiently small lengths of α_1, α_2, and α_3. Use

$$\lim_{x \to 0^+} \sinh^{-1}(\sinh x \cosh(\sinh^{-1}(\coth x))) = \sinh^{-1} 1 \approx 0.88137, \tag{8.5}$$

and $\ell(\alpha_n) \leq \frac{C_2}{n^2}$ for $n \geq 1$ and for level n cuffs α_n, to conclude that the quantity

$$D = \sinh^{-1}(\sinh A \cosh(\sinh^{-1}(\coth A)))$$

such that $A = \max\{\frac{\ell(\alpha_2)}{2}, \ell(p)\}$ in Lemma B.3 is uniformly bounded for $f(\tilde{P})$.

By Lemma B.3(2), $d/dx(\tanh^{-1} x) = 1/(1-x^2)$, $\tanh^{-1} x \geq x$ for $x \geq 0$, $\ell(p) \to 0$, and $x \lesssim \tanh x$ for small $x > 0$ using the concavity of $\tanh x$,

$$\begin{aligned}(\frac{\partial v_P}{\partial x})^2 &= y^2[\frac{1}{\tanh^{-1}(\tanh \ell(p) \cosh x)}]^4[\frac{\tanh \ell(p) \sinh x}{1 - [\tanh \ell(p) \cosh x]^2}]^2 \\ &\lesssim \frac{y^2}{\tanh^2 \ell(p)} \tanh^2 x \operatorname{sech}^2 x \lesssim \frac{y^2}{\ell(p)^2} \tanh^2 x \operatorname{sech}^2 x,\end{aligned}$$

and

$$(\frac{\partial v_P}{\partial y})^2 = [\frac{1}{\tanh^{-1}(\tanh \ell(p) \cosh x)}]^2 \lesssim \frac{1}{\ell(p)^2} \operatorname{sech}^2 x.$$

By [11, Theorem 2.3.4(ii)], $\sinh(\cosh^{-1} x) < x$ for $x > 1$, and $x \lesssim \tanh x$ for small $x > 0$ using the concavity of $\tanh x$,

$$\ell(p) \sinh \ell(o_{1,2}) = \ell(p) \sinh(\cosh^{-1}(\frac{1}{\tanh \frac{\ell(\alpha_2)}{2} \tanh \ell(p)})) \lesssim \frac{1}{\ell(\alpha_2)}. \tag{8.6}$$

We integrate, use equations (8.4) and (8.6), and Lemma B.3(3) to get

$$\begin{aligned}\iint_{f(\tilde{P})}(\frac{\partial v_P}{\partial x})^2 &\lesssim \frac{1}{\ell(p)^2}\int_0^{\ell(o_P)}\int_0^{d_h^P(x)} y^2\tanh^2 x\,\mathrm{sech}^2\, x dy dx\\ &\lesssim \ell(p)\int_0^{\ell(o_P)}\sinh x\tanh x dx < \ell(p)\int_0^{\ell(o_P)}\cosh x dx\\ &< \ell(p)\sinh\ell(o_{1,2}) \lesssim \frac{1}{\ell(\alpha_2)}.\end{aligned}$$

In addition, by Lemma B.3(3) and $\int_0^\infty \mathrm{sech}\, x dx = \frac{\pi}{2}$ we get

$$\begin{aligned}\iint_{f(\tilde{P})}(\frac{\partial v_P}{\partial y})^2 &\lesssim \frac{1}{\ell(p)^2}\int_0^{\ell(o_P)}\int_0^{d_h^P(x)}\mathrm{sech}^2\, x dy dx\\ &\lesssim \frac{1}{\ell(p)}\int_0^{\ell(o_P)}\mathrm{sech}\, x dx \lesssim \frac{1}{\ell(p)}.\end{aligned}$$

The above, together with Lemma B.3(4), gives

$$\iint_{f(\tilde{P})}(\frac{\partial v_P}{\partial x})^2+(\frac{\partial v_P}{\partial y})^2 \lesssim \frac{1}{\ell(\alpha_2)}+\frac{1}{\ell(p)} \lesssim \frac{1}{\ell(\alpha_1)}+\frac{1}{\ell(\alpha_2)}.$$

The orthogeodesic from the point $a_1 \cap o_{2,3}$ to $o_{1,3}$ divides P_q into quadrilaterals Q and S adjacent to α_1 and α_3 (see Figure 8.2). By the analogous notation and derivations, we obtain

$$\begin{aligned}\iint_{f(\tilde{P})\cup f(\tilde{R})}(\frac{\partial v}{\partial x})^2+(\frac{\partial v}{\partial y})^2 &\lesssim \frac{1}{\ell(\alpha_1)}+\frac{1}{\ell(\alpha_2)},\\ \iint_{f(\tilde{Q})\cup f(\tilde{S})}(\frac{\partial v}{\partial x})^2+(\frac{\partial v}{\partial y})^2 &\lesssim \frac{1}{\ell(\alpha_1)}+\frac{1}{\ell(\alpha_3)}.\end{aligned} \tag{8.7}$$

Lemma C.1 enables us to estimate the Dirichlet integrals of the foliations of quadrilaterals P, Q, R, and S in the front of Π from above using the inequality [2]

$$\iint_{\tilde{\Omega}}[(\frac{\partial(v\circ f)}{\partial\xi})^2+(\frac{\partial(v\circ f)}{\partial\eta})^2]d\xi d\eta \le k_0\iint_{f(\tilde{\Omega})}[(\frac{\partial v}{\partial x})^2+(\frac{\partial v}{\partial y})^2]dxdy, \tag{8.8}$$

where $\tilde{\Omega}$ is $\tilde{P}$, $\tilde{Q}$, $\tilde{R}$, or $\tilde{S}$.

To summarize the next step, we define an integrable partial measured foliation $\mathscr{F}$ supported on the front of the Cantor tree surface X_C by scaling the partial foliations defined

by v_P, v_Q, v_R, and v_S in every pair of pants in the decomposition of X_C in order for the transverse measures on the common boundaries of any two quadrilaterals to agree. The transverse measures on the "vertical" boundaries of the quadrilaterals P, Q, R, and S that are given by integrating the differentials dv_P, dv_Q, dv_R, and dv_S are proportional to the hyperbolic lengths, and on each vertical boundary, the corresponding measure equals to 1.

Let $P^{n,j}$, $Q^{n,j}$, $R^{n,j}$, and $S^{n,j}$ be the Lambert quadrilaterals P, Q, R, and S in the front of a level n pair of pants $\Pi^{n,j}$ of X with the front of a level $n-1$ cuff α_{n-1}^j as a boundary for $n \geq 1$ and for each $1 \leq j \leq 2^n$ (see that $\alpha_0^1 = \alpha_0^2 = \alpha_0$). Define the geodesic arcs p_{n-1}^j and q_{n-1}^j to be in the front hexagon of the pair of pants as the intersections $P^{n,j} \cap \alpha_{n-1}^j$ and $Q^{n,j} \cap \alpha_{n-1}^j$. We define the *relative lengths* of p_{n-1}^j and q_{n-1}^j by

$$\ell_{n-1,j}^0 = \frac{\ell(p_{n-1}^j)}{\ell(\alpha_{n-1}^j)/2} \quad \text{and} \quad \ell_{n-1,j}^1 = \frac{\ell(q_{n-1}^j)}{\ell(\alpha_{n-1}^j)/2}.$$

Let $v_P^{n,j}$, $v_Q^{n,j}$, $v_R^{n,j}$, and $v_S^{n,j}$ be the partial measured foliations of $f(\tilde{P}^{n,j})$, $f(\tilde{Q}^{n,j})$, $f(\tilde{R}^{n,j})$, and $f(\tilde{S}^{n,j})$ for $n \geq 1$ and for each $1 \leq j \leq 2^n$ as the foliations v_P, v_Q, v_R, and v_S for $f(\tilde{P})$, $f(\tilde{Q})$, $f(\tilde{R})$, and $f(\tilde{S})$.

Each pair of pants $\Pi^{n,j}$ starting from the top cuff α_0 can be reached by a unique path of n consecutive cuffs. In addition, at each cuff in the path, with the exception of the last cuff, we can choose either p or q depending on whether the next cuff is to the left or the right. The new function w that defines the partial measured foliation $\mathscr{F}$ is obtained by multiplying the foliations of $f(\tilde{P}^{n,j})$ and $f(\tilde{R}^{n,j})$ with the product of the relative lengths of the corresponding choices of p's and q's on the path of cuffs times the relative length of p_n^j (see Figure 8.4), and by multiplying the foliations of $f(\tilde{Q}^{n,j})$ and $f(\tilde{S}^{n,j})$ with the product of the relative lengths of the corresponding choices of p's and q's on the path of cuffs times the relative length of q_n^j. In this fashion, the transverse measures of the foliations of adjacent quadrilaterals on the common side of the quadrilaterals given by the function w are equal, and w defines a partial measured foliation supported on the front side of X_C.

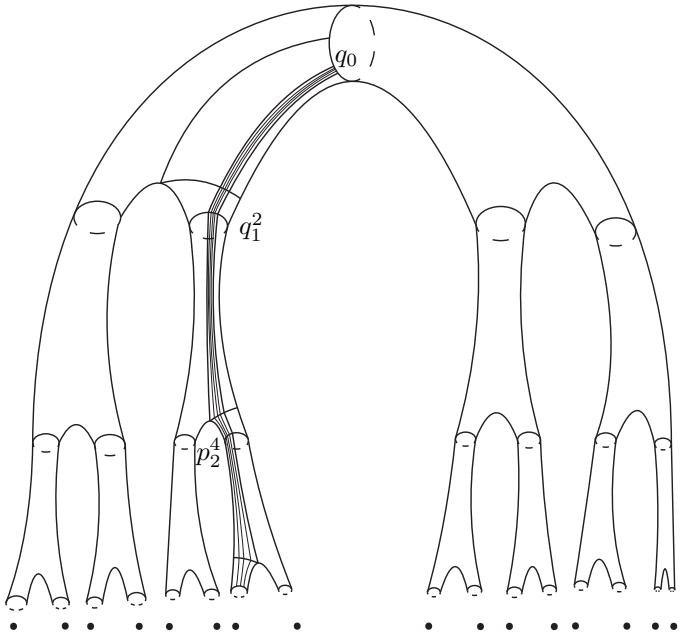

Figure 8.4: Illustration of how to choose p's and q's for the product of relative lengths.

The function w induces the measure on α_0 of mass 1. The total mass of transverse measure on α_n^j is

$$\Pi_{k=0}^{n-1}\ell_{k,j}^{i_k}, \tag{8.9}$$

where $i_k \in \{0,1\}$ depending on the path of consecutive cuffs from α_0 to α_n^j.

Let $T = \sum_{n=1}^{\infty}\frac{1}{n^2} < \infty$. From Appendix B.1,

$$\frac{1}{2}e^{-\frac{C_2}{(k+1)^2}} \leq \ell_{k,j}^{i_k} \leq \frac{1}{2}e^{\frac{C_2}{(k+1)^2}}$$

for $0 \leq k \leq n-1$. Use the above inequalities for $0 \leq k \leq n-1$ to obtain

$$\frac{1}{2^n}e^{-C_2T} \leq \frac{1}{2^n}e^{-C_2\sum_{k=1}^{n}\frac{1}{k^2}} \leq \Pi_{k=0}^{n-1}\ell_{k,j}^{i_k} \leq \frac{1}{2^n}e^{C_2\sum_{k=1}^{n}\frac{1}{k^2}} \leq \frac{1}{2^n}e^{C_2T}.$$

That means

$$\Pi_{k=0}^{n-1}\ell_{k,j}^{i_k} \asymp \frac{1}{2^n}. \tag{8.10}$$

Therefore, the transverse measures of $\mathscr{F}$ on p_n^j and q_n^j are both asymptotic to $\frac{1}{2^n}$.

By (8.10), (8.7), $\ell(\alpha_n^j) \geq \frac{n^r}{2^n}$, and the symmetry of a pair of pants, the Dirichlet integral

of w over any level n pair of pants $\Pi^{n,j}$ equals

$$\begin{aligned}
&2\left[\iint_{f(\tilde{P}^{n,j})\cup f(\tilde{R}^{n,j})}(\frac{\partial w}{\partial x})^2+(\frac{\partial w}{\partial y})^2+\iint_{f(\tilde{Q}^{n,j})\cup f(\tilde{S}^{n,j})}(\frac{\partial w}{\partial x})^2+(\frac{\partial w}{\partial y})^2\right]\\
&\leq K_1\left[(\mu_P^{n,j})^2\left(\frac{1}{\ell(\alpha_1)}+\frac{1}{\ell(\alpha_2)}\right)+(\mu_Q^{n,j})^2\left(\frac{1}{\ell(\alpha_1)}+\frac{1}{\ell(\alpha_3)}\right)\right]\\
&\leq K_2[\max\{\mu_P^{n,j},\mu_Q^{n,j}\}]^2\cdot\frac{2^n}{n^r}\leq K_3\frac{1}{2^{2n}}\frac{2^n}{n^r}=K_3\frac{1}{2^n\cdot n^r}
\end{aligned}$$

for some $K_1, K_2, K_3 > 0$, where $\mu_P^{n,j}$ and $\mu_Q^{n,j}$ are the transverse measures of $\mathscr{F}$ on p_n^j and q_n^j.

Since there are 2^n level n pairs of pants, we have for some $K > 0$ that

$$D_{X_C}(\mathscr{F})\leq K\sum_{n=1}^{\infty}\frac{1}{n^r}<\infty.$$

By construction, both rays of every leaf in $\mathscr{F}$ leave every compact subset of X_C. Therefore $X_C \notin O_G$, and this finishes the proof of Theorem 8.1.

We proceed to assume that $\tilde{X}_C$ is the blooming Cantor tree surface with the properties stated in Theorem 1.2 . Assume, without loss of generality, no surface of genus at most C and two boundaries is attached to α_0. Refer to the front of the surface as $\tilde{X}$ for simplicity. Consider a geodesic pants decomposition of a surface with genus at most C and two geodesic boundaries, denoted by $S_{g,2}$. For each pair of pants in the decomposition of $S_{g,2}$, a collection of closed geodesic arcs separates it into two symmetric sides permuted by an orientation-reversing isometry. Choose any pair of pants in the decomposition of $S_{g,2}$ and choose one of its sides to be its front. Define the front of each adjacent pair of pants in the decomposition of $S_{g,2}$ as the side that is adjacent to the front of the chosen pair of pants. Repeat this procedure inductively until the front of each pair of pants in the decomposition of $S_{g,2}$ is defined. We define the front of $S_{g,2}$ as the union of the fronts of the pairs of pants in its decomposition. Denote by S_n^j the subset of $\tilde{X}$ that is the union of the front of a level n pair of pants and the fronts of the sub-surfaces possibly attached to each of its level n boundaries with genus at most C and two geodesic boundaries for $n \geq 1$ and for each $1 \leq j \leq 2^n$.

Decompose S_n^j into at most $8C+2$ sub-regions, half of which are examples of $P \cup R$ regions, while the rest are examples of $Q \cup S$ regions. Let $\mathscr{F}$ be a partial measured foliation of $\tilde{X}$ modified by a function w that is defined similarly as in Theorem 8.1. By a similar argument used for Theorem 8.1, the transverse measures of $\mathscr{F}$ on p_n^j and q_n^j are both asymptotic to $\frac{1}{2^n}$. Therefore, from the estimates in (8.7), Appendix C.1, and inequality $\ell(\alpha_n^j) \geq C_1 \frac{n^r}{2^n}$ for $n \geq 1$ and for each $1 \leq j \leq 2^{n+1}$,

$$\iint_{S_n^j} (\frac{\partial w}{\partial x})^2 + (\frac{\partial w}{\partial y})^2 \leq K \frac{1}{2^{2n}} \frac{2^n}{n^r} = K \frac{1}{2^n \cdot n^r}.$$

for some $K > 0$. Since there are 2^n sub-surfaces S_n^j for $n \geq 1$ on both the front and back of the surface $\tilde{X}_C$, we have for some $K > 0$ that

$$D_{\tilde{X}_C}(\mathscr{F}) \leq K \sum_{n=1}^{\infty} \frac{1}{n^r} < \infty.$$

By construction, both rays of every leaf in $\mathscr{F}$ leave every compact subset of $\tilde{X}_C$. Therefore $\tilde{X}_C \notin O_G$, and this finishes the proof of Theorem 8.2.

Appendix A

Let $\{g_n\}$ be a nested sequence of geodesics in $\mathbb{D}$. Assume each g_n has exactly one ideal endpoint on S^1 in common with g_{n+1} and that no three consecutive geodesics g_n have an ideal endpoint in common. The space between g_n and g_{n+1} in $\mathbb{D}$ is called a *wedge* W_n for each $n \geq 1$. The shared ideal endpoint of g_n and g_{n+1} is the *vertex* of wedge W_n.

For any fixed point P_1 on g_1, there is a unique concatenation h of horocyclic arcs h_n in wedges W_n that connects the sides of every g_n starting at P_1. In the appendix, we prove that the nested sequence of geodesics $\{g_n\}$ accumulates to a single point on S^1 if and only if the piecewise horocyclic path h has infinite length. In addition, we also prove formulas that give the lengths of the horocyclic arcs h_n inside wedges W_n in terms of the shears of the geodesics up to and including g_n. Both results use the ideas from [17, Theorem C], and we give a proof for the convenience of the reader.

Proposition A.1. *Let $\{g_n\}_{n=1}^{\infty}$ be a nested sequence of geodesics and h a piecewise horocyclic path as above. Then the nested sequence $\{g_n\}_n$ accumulates to a single point on S^1 if and only if h has infinite length.*

Proof. Assume that the piecewise horocyclic path h has a finite length. If the geodesics g_n accumulates to a single point on S^1, then the path h contains a sequence of points that converges toward that point on S^1. Since the distance from P_1 to any point on the ideal boundary is infinite, it means that h has an infinite length which is a contradiction. Thus, g_n does not accumulate to a single point on S^1.

To prove the converse, assume that the geodesics g_n converge to a geodesic $g^\star$ in $\mathbb{D}$. Then the goal will be to prove that h has a finite length. Since the geodesics g_n accumulate to the

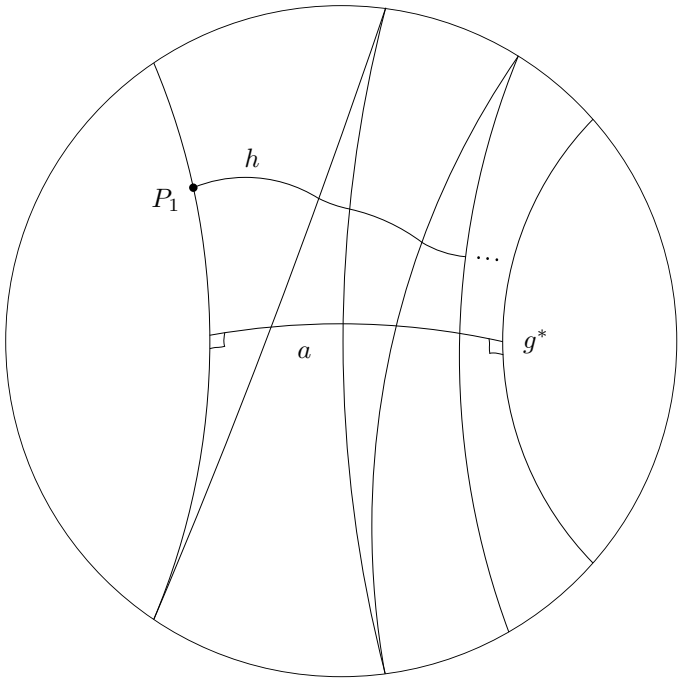

Figure A.1: The piecewise horocyclic arc h and the orthogeodesic a.

geodesic $g^\star$, we can find an orthogeodesic arc a from g_1 to $g^\star$. The length of a is finite, and its length compares to the length of h (see Figure A.1).

Let W_n be the wedge between g_n and g_{n+1}. Call $a_n = a \cap W_n$ and $h_n = h \cap W_n$. Denote the geodesic arc on g_n whose endpoints are $a \cap g_n$ and $h \cap g_n$ by d_n.

Let h'_n be the horocyclic arc from $g_n \cap a_n$ to g_{n+1} centered at the vertex of wedge W_n. Let b_n be the geodesic subarc of g_{n+1} between $a_n \cap g_{n+1}$ and $h'_n \cap g_{n+1}$. Let c_n be the geodesic arc that connects the endpoints of h'_n. The geodesic arcs a_n, b_n, and c_n form the three sides of a geodesic triangle. Let α_n be the angle in this triangle opposite a_n, and let β_n the angle opposite to b_n (see Figure A.2). The sine formula gives

$$\frac{\sinh \ell(a_n)}{\sin \alpha_n} = \frac{\sinh \ell(b_n)}{\sin \beta_n}. \tag{11}$$

We prove that $0 < \alpha_l \leq \alpha_n \leq \alpha_u < \pi$ for all n. Use a Möbius function to map the wedge W_n in $\mathbb{D}$ to the wedge in $\mathbb{H}$ whose vertex is ∞ and whose boundary geodesics $(0, \infty)$ and $(1, \infty)$ are images of g_n and g_{n+1}, respectively. Denote the images of a_n, b_n, c_n, h'_n and α_n by the same letters (see Figure A.3). The length $\ell(a_n)$ is bounded above by $\ell(a) < \infty$ for

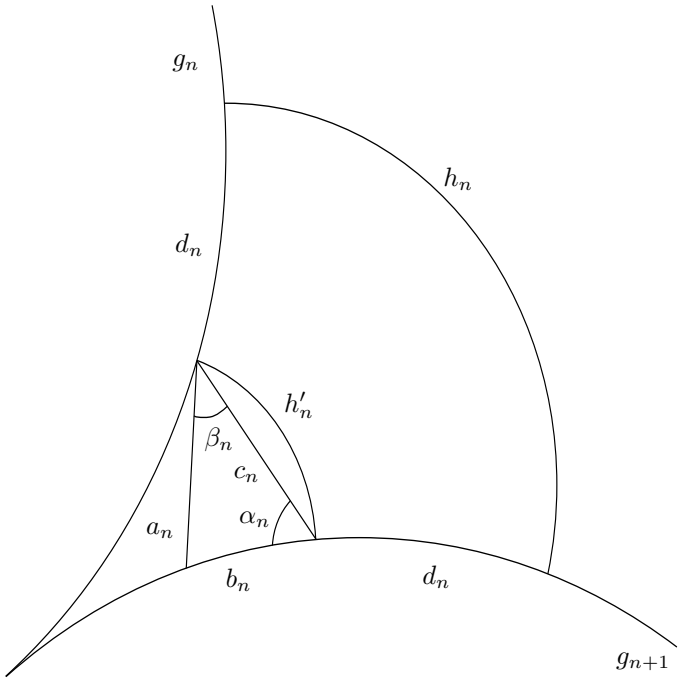

Figure A.2: The comparison between a_n and h_n.

all n. Consequently, there is a positive lower bound $y_0 > 0$ on the heights of the points in a_n for each n. Then, the horocyclic arc h'_n has Euclidean height at least $y_0 > 0$. Also, the Euclidean circle that contains the geodesic arc c_n has a center of $1/2 \in \mathbb{R}$ and a radius greater than y_0. By elementary Euclidean geometry, these bounds imply the existence of $0 < \alpha_l < \alpha_u < \pi$ such that $\alpha_n \in [\alpha_l, \alpha_u]$ for all n.

From (11) and the fact that $\alpha_l \leq \alpha_n \leq \alpha_u$, we conclude that

$$\ell(b_n) \leq C\ell(a_n) \tag{12}$$

for some constant $C > 0$ and for $n \geq 1$. By Figure A.3 and inequality (12), we obtain

$$\ell(d_{n+1}) = \ell(d_n) + \ell(b_n) \leq \ell(d_n) + C\ell(a_n)$$

which implies

$$\ell(d_{n+1}) \leq \ell(d_1) + C\sum_{i=1}^{n} \ell(a_i) \leq \ell(d_1) + C\ell(a). \tag{13}$$

The notation $a \asymp b$ means there exists positive constants $k_1, k_2 > 0$ such that $k_1 \leq \frac{a}{b} \leq k_2$.

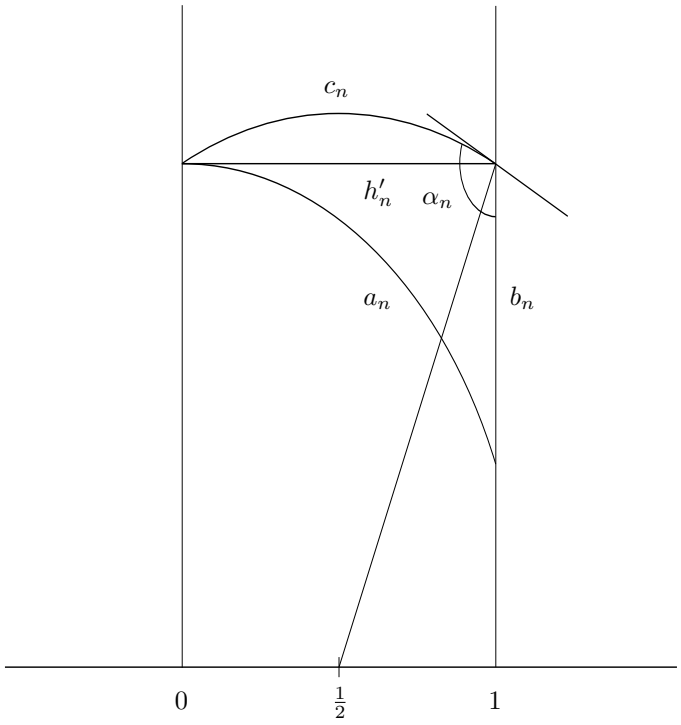

Figure A.3: The wedge with vertex ∞.

Using (13), we obtain $\ell(h'_n) \asymp \ell(h_n)$. Observe

$$\ell(c_n) \leq \ell(a_n) + \ell(b_n) \leq (1+C)\ell(a_n) \leq (1+C)\ell(a).$$

This observation and the fact that h'_n and c_n share endpoints imply $\ell(h'_n) \asymp \ell(c_n)$. Therefore

$$\ell(h) = \sum_{n=1}^{\infty} \ell(h_n) \asymp \sum_{n=1}^{\infty} \ell(h'_n) \asymp (1+C) \sum_{n=1}^{\infty} \ell(a_n) = (1+C)\ell(a) < \infty.$$

This completes the proof of the proposition. □

We find the length of the horocyclic arc h_n in terms of the shears $s(g_i)$ on the geodesics g_i from $i = 1$ to $i = n$. Consider two wedges, W_1 and W_2, which share a common geodesic edge g_2 such that the vertices of the wedges are the endpoints of g_2. The wedge W_1 is the space between geodesics g_1 and g_2, and the wedge W_2 is the space between geodesics g_2 and g_3. If g_2 is a geodesic from the initial point of g_1 to the terminal point of g_3, the pair of wedges (W_1, W_2) is said to be *left-open* (see the left side of Figure A.4). Otherwise, if the geodesic g_2 connects the initial point of g_3 and the terminal point of g_1, the pair of wedges

(W_1, W_2) is *left-closed* (see right side of Figure A.4).

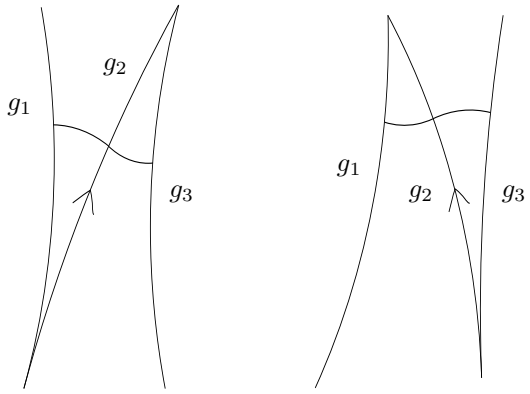

Figure A.4: A left-open and a left-closed pair of wedges (W_1, W_2).

Lemma A.2. *Let (W_1, W_2) be a pair of adjacent wedges and let h_1 be a horocyclic arc orthogonal to and connecting the boundary sides of W_1. Let $s(g_2)$ be the shear along the common boundary geodesic g_2 of (W_1, W_2) of the ideal quadrilateral with vertices equal to the endpoints of g_1 and g_3. Let h_2 be the horocyclic arc in W_2 orthogonal to its boundary that continues h_1.*

If (W_1, W_2) is left-open then

$$\ell(h_2) = \frac{e^{s(g_2)}}{\ell(h_1)},$$

where $\ell(h_1)$ and $\ell(h_2)$ are the lengths of h_1 and h_2.

If (W_1, W_2) is left-closed then

$$\ell(h_2) = \frac{e^{-s(g_2)}}{\ell(h_1)}.$$

Proof. We map a left-closed wedge (W_1, W_2) into $\mathbb{H}$ so that the common boundary geodesic of the wedges gets mapped to $g_2 = (0, \infty)$, and the endpoint of g_1 not on g_2 gets mapped to -1. Since $s(g_2)$ is the value of the shear on geodesic g_2, we have that the geodesic g_3 gets mapped to $(0, e^{s(g_2)})$. The horocyclic arc between g_1 and g_2 is a horizontal Euclidean line segment that meets g_2 at the point iy_1 (see Figure A.5).

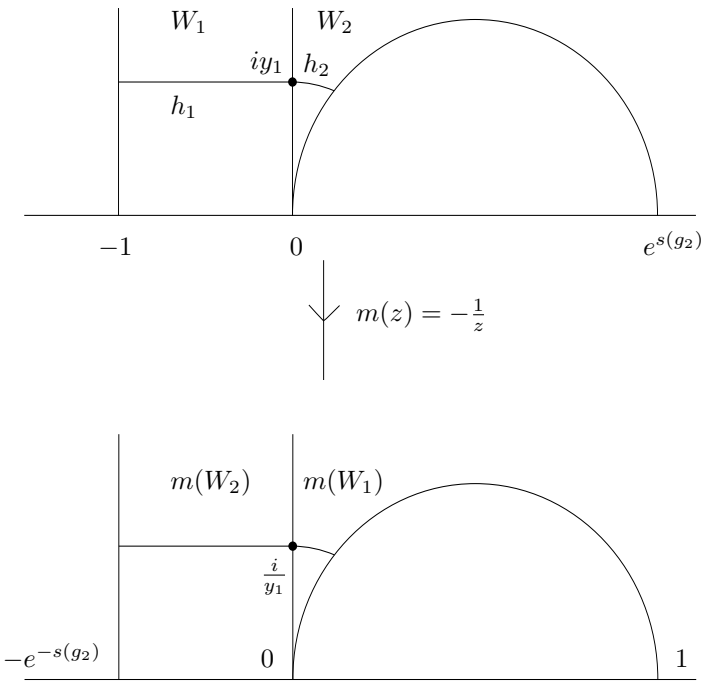

Figure A.5: The left-closed pair of wedges with the vertex ∞.

We calculate the length $l(h_1)$ to be $\frac{1}{y_1}$. Define the Mobius map $m(z) = -\frac{1}{z}$. The Mobius m sends the geodesic g_2 to itself, and g_3 to the geodesic $m(g_3) = (-e^{-s(g_2)}, \infty)$. The horocyclic arc h_2 between geodesics g_2 and g_3 gets mapped to the horizontal Euclidean line segment of height $\frac{1}{y_1}$ between $m(g_3)$ and $m(g_2) = g_2$. Therefore,

$$\ell(h_2) = \ell(m(h_2)) = e^{-s(g_2)} y_1 = \frac{e^{-s(g_2)}}{l(h_1)}.$$

The length of h_2 for left-open wedges is determined similarly. □

We find the length of the nth horocyclic arc h_n in terms of the length $l(h_1)$ of the first horocyclic arc and in terms of the shears of all of the geodesics up to and including g_n.

Proposition A.3. *Let $\{g_n\}_{n=1}^{\infty}$ be the above nested family of geodesics and let $s_n = s(g_n)$ be the corresponding shears. Let h be a curve obtained by concatenation of horocyclic arcs h_n orthogonal to and connecting two boundary geodesics of each wedge W_n starting at a point $P_1 \in g_1$. Choose $P_1 \in g_1$ such that the horocyclic arc $h_1 = h \cap W_1$ has length e^{-s_1}. Then, for n odd,*

$$\ell(h_n) = e^{-s_1 - s_2 - \cdots - s_n}$$

and, for n even,

$$\ell(h_n) = e^{s_1+s_2+\cdots+s_n}$$

Proof. Consider the wedge W_n such that $n > 1$. By Lemma A.2, and the fact that the pair of adjacent wedges (W_1, W_2) is left-open, we have $l(h_2) = \frac{e^{s_2}}{l(h_1)} = e^{s_1+s_2}$. Also, by Lemma A.2, since the pair of adjacent wedges (W_2, W_3) is left-closed, we have $L(h_3) = \frac{e^{-s_3}}{l(h_2)} = e^{-s_1-s_2-s_3}$. The result follows by induction. □

Appendix B

Let Π be a geodesic pair of pants with boundaries α_1, α_2, and α_3. The following observations concerning Π are exactly the same as in Section 3. Let $o_{i,j}$ be the orthogeodesic arc between α_i and α_j, for $i, j \in \{1, 2, 3\}$ such that $i \neq j$. The union $o_{1,2} \cup o_{1,3} \cup o_{2,3}$ separates Π into front and back hexagons H_1 and H_2 with geodesic boundaries. Let a_1 be the orthogeodesic from α_1 to $o_{2,3}$ that separates H_1 into two right-angled pentagons and divides α_1 in H_1 from left to right into the sub-arcs p and q (see Figure 8.2). Call P_p the pentagon containing p (see Figure 8.2), and P_q the pentagon containing q. The orthogeodesic b_1 from $a_1 \cap o_{2,3}$ to $o_{1,2}$ divides P_p into quadrilaterals P and R adjacent to α_1 and α_2. Let o_P be the sub-arc of $o_{1,2}$ in P and let o_R be the sub-arc of $o_{1,2}$ in R (see Figure 8.2).

Observe that

$$\frac{d}{dx}\left(\frac{\sinh x}{A+\cosh x}\right)|_{x=0} = \frac{1}{A+1} \; and \; \frac{d}{dx}\left(\tanh\left(\frac{x}{2A}\right)\right)|_{x=0} = \frac{1}{2A}.$$

It is also true that

$$\frac{1}{A+1} > \frac{1}{2A}$$

if and only if $A > 1$ or $A \in (-1, 0)$. Let $A > 0$. For small $x > 0$, we get $A > 1$ if and only if

$$\frac{\sinh x}{A+\cosh x} > \tanh\left(\frac{x}{2A}\right), \tag{14}$$

with equality if and only if $A = 1$.

Recall that the *relative lengths* associated with α_1 in the front of Π is

$$\ell^0 = \frac{\ell(p)}{\frac{\ell(\alpha_1)}{2}} \text{ and } \ell^1 = \frac{\ell(q)}{\frac{\ell(\alpha_1)}{2}}.$$

Let $\ell = \ell^0$ or $\ell = \ell^1$.

Lemma B.1. *Assume* $\frac{C_2}{(n+1)^2} \geq \max\{\ell(\alpha_2), \ell(\alpha_3)\}$ *for a positive constant* C_2 *and for some* $n \geq 1$. *Moreover, assume that* $\ell(\alpha_1) > 0$ *is small enough so that inequality (14) holds when* $x = \frac{\ell(\alpha_1)}{2}$. *Then, any relative length* ℓ *associated with* α_1 *in the front of* Π *satisfies*

$$\frac{1}{2}e^{-\frac{C_2}{(n+1)^2}} \leq \ell \leq \frac{1}{2}e^{\frac{C_2}{(n+1)^2}}.$$

Proof. Using a formula for right-angled pentagons [9, Theorem 7.18.1],

$$\tanh \ell(p) \cosh \ell(o_{1,2}) \tanh \frac{\ell(\alpha_2)}{2} = 1. \tag{15}$$

A formula for right-angled hexagons [9, Theorem 7.19.2], gives

$$\cosh \ell(o_{1,2}) = \frac{\cosh \frac{\ell(\alpha_3)}{2}}{\sinh \frac{\ell(\alpha_1)}{2} \sinh \frac{\ell(\alpha_2)}{2}} + \coth \frac{\ell(\alpha_1)}{2} \coth \frac{\ell(\alpha_2)}{2}. \tag{16}$$

Use (14), (15), and (16) to obtain for the relative length ℓ^0 that

$$\begin{aligned}
\ell^0 &= \frac{2}{\ell(\alpha_1)} \tanh^{-1} \left(\frac{\sinh\left(\frac{\ell(\alpha_1)}{2}\right)}{\frac{\cosh\left(\frac{\ell(\alpha_3)}{2}\right)}{\cosh\left(\frac{\ell(\alpha_2)}{2}\right)} + \cosh\left(\frac{\ell(\alpha_1)}{2}\right)} \right) \\
&\geq \frac{1}{2} \left[\frac{\cosh\left(\min\left\{\frac{\ell(\alpha_2)}{2}, \frac{\ell(\alpha_3)}{2}\right\}\right)}{\cosh\left(\max\left\{\frac{\ell(\alpha_2)}{2}, \frac{\ell(\alpha_3)}{2}\right\}\right)} \right] \\
&> \frac{e^{-\max\{\ell(\alpha_2), \ell(\alpha_3)\}}}{2}.
\end{aligned}$$

Fix a positive constant C_2 and fix some value of $n \geq 1$. From the assumption that $\frac{C_2}{(n+1)^2} \geq \max\{\ell(\alpha_2), \ell(\alpha_3)\}$, the above is greater than or equal to

$$\frac{1}{2}e^{-\frac{C_2}{(n+1)^2}}.$$

Similarly, we obtain the same lower bound for ℓ^1 for $C_2 > 0$ and for $n \geq 1$. Let

$$B = \frac{\sinh(\frac{\ell(\alpha_1)}{2})}{\frac{\cosh(\frac{\ell(\alpha_3)}{2})}{\cosh(\frac{\ell(\alpha_2)}{2})} + \cosh(\frac{\ell(\alpha_1)}{2})}.$$

Use (14) and $\cosh x$ is increasing to obtain

$$\begin{aligned} B &< \tanh\left(\frac{\frac{\ell(\alpha_1)}{2}}{2\left(\frac{\cosh(\frac{\ell(\alpha_3)}{2})}{\cosh(\frac{\ell(\alpha_2)}{2})}\right)}\right) \\ &= \tanh\left([\frac{\cosh\left(\max\left\{\frac{\ell(\alpha_2)}{2}, \frac{\ell(\alpha_3)}{2}\right\}\right)}{\cosh\left(\min\left\{\frac{\ell(\alpha_2)}{2}, \frac{\ell(\alpha_3)}{2}\right\}\right)}]\frac{\ell(\alpha_1)}{4}\right) \end{aligned}$$

if $\ell(\alpha_3) < \ell(\alpha_2)$, and

$$\begin{aligned} B &\leq \frac{\sinh(\frac{\ell(\alpha_1)}{2})}{1 + \cosh(\frac{\ell(\alpha_1)}{2})} \\ &= \tanh\left(\frac{\frac{\ell(\alpha_1)}{2}}{2(1)}\right) \\ &\leq \tanh\left([\frac{\cosh\left(\max\left\{\frac{\ell(\alpha_2)}{2}, \frac{\ell(\alpha_3)}{2}\right\}\right)}{\cosh\left(\min\left\{\frac{\ell(\alpha_2)}{2}, \frac{\ell(\alpha_3)}{2}\right\}\right)}]\frac{\ell(\alpha_1)}{4}\right) \end{aligned}$$

if $\ell(\alpha_3) \geq \ell(\alpha_2)$. Therefore,

$$\begin{aligned} \ell^0 &= \frac{2}{\ell(\alpha_1)} \tanh^{-1}(B) \\ &\leq \frac{2}{\ell(\alpha_1)} \tanh^{-1}\left(\tanh\left([\frac{\cosh\left(\max\left\{\frac{\ell(\alpha_2)}{2}, \frac{\ell(\alpha_3)}{2}\right\}\right)}{\cosh\left(\min\left\{\frac{\ell(\alpha_2)}{2}, \frac{\ell(\alpha_3)}{2}\right\}\right)}]\frac{\ell(\alpha_1)}{4}\right)\right) \\ &< \frac{1}{2} e^{\frac{C_2}{(n+1)^2}} \end{aligned}$$

for $C_2 > 0$ and for $n \geq 1$. Get the same upper bound for ℓ^1 similarly for $C_2 > 0$ and for $n \geq 1$. □

Remark B.2. *Lemma B.1 is still true when $\ell(\alpha_1)$ and $\ell(\alpha_3)$ are close and α_2 is a puncture.*

We will require the following estimates. Refer to the beginning of Appendix B and Figure

8.3 for the definitions of Π and $f(\tilde{P})$.

Lemma B.3. *We prove inequalities 1-3 in $f(\tilde{P})$ and inequality 4 in Π. Let $A = \max\{\frac{\ell(\alpha_2)}{2}, \ell(p)\}$.*

1. *$\ell(b_1) \leq D$ for some $D > 0$, depending on A.*

2. *Assume $0 \leq x \leq \ell(o_P)$. Then*

$$\frac{1}{1 - [\tanh \ell(p) \cosh x]^2} \leq c$$

   for some $c > 0$, depending on A.

3. *Assume $0 \leq x \leq \ell(o_P)$. Then*

$$\tanh^{-1}(\tanh \ell(p) \cosh x) \leq c \tanh \ell(p) \cosh x$$

   for some $c > 0$, depending on A.

4. *If $\cosh \frac{\ell(\alpha_3)}{2} \leq 2$, then $\ell(p) \gtrsim \ell(\alpha_1)$.*

Proof. Let s be the length of the geodesic sub-arc of $o_{2,3}$ from a_1 to α_2. By a formula [9, Theorem 7.18.1] for right-angled pentagons,

$$\sinh \ell(a_1) \sinh \ell(p) = \cosh \frac{\ell(\alpha_2)}{2} \text{ and } \sinh s \sinh \frac{\ell(\alpha_2)}{2} = \cosh \ell(p).$$

A formula for Lambert quadrilaterals [11, Theorem 2.3.1(v)] gives

$$\sinh \ell(b_1) = \sinh \ell(p) \cosh \ell(a_1) \text{ and } \sinh \ell(b_1) = \sinh \frac{\ell(\alpha_2)}{2} \cosh s.$$

We will use the fact that cosh, sinh, and $\sinh^{-1}$ are increasing and positive on $\mathbb{R}_+$. Let $D = \sinh^{-1}(\sinh A \cosh(\sinh^{-1}(\coth A)))$. If $\ell(p) \leq \frac{\ell(\alpha_2)}{2}$, then

$$\begin{aligned} \ell(b_1) &= \sinh^{-1}(\sinh(\frac{\ell(\alpha_2)}{2}) \cosh(\sinh^{-1}(\frac{\cosh(\ell(p))}{\sinh(\frac{\ell(\alpha_2)}{2})}))) \\ &\leq \sinh^{-1}(\sinh(A) \cosh(\sinh^{-1}(\coth(A)))). \end{aligned} \tag{17}$$

Otherwise,

$$\begin{aligned}\ell(b_1) &= \sinh^{-1}(\sinh(\ell(p))\cosh(\sinh^{-1}(\frac{\cosh(\frac{\ell(\alpha_2)}{2})}{\sinh(\ell(p))}))) \\ &\leq \sinh^{-1}(\sinh(A)\cosh(\sinh^{-1}(\coth(A)))).\end{aligned} \tag{18}$$

Therefore, by (17), (18), and the definition of D, we obtain

$$\ell(b_1) \leq D. \tag{19}$$

From two formulas [11, Theorem 2.3.1(i) and (iii)] for Lambert quadrilaterals and basic computations,

$$\tanh \ell(b_1) = \tanh \ell(p) \cosh \ell(o_P). \tag{20}$$

Consider x such that $0 \leq x \leq \ell(o_P)$. Use $\cosh x$ and $\tanh^{-1} x$ are increasing, (20), and (19) to obtain

$$\tanh^{-1}(\tanh \ell(p) \cosh x) \leq \tanh^{-1}(\tanh \ell(p) \cosh \ell(o_P)) = \ell(b_1) \leq D,$$

$$\frac{1}{1 - [\tanh \ell(p) \cosh x]^2} \leq \cosh^2 D.$$

This implies $\tanh \ell(p) \cosh x \leq \tanh D$. Using the convexity of $\tanh^{-1} x$ on $[0, \tanh D]$, we get

$$\tanh^{-1}(\tanh \ell(p) \cosh x) \leq E \tanh \ell(p) \cosh x.$$

for some $E > 0$, where the size of E depends on how small $\tanh D$ is. Let $c = \max\{\cosh^2(D), E\}$ to attain inequalities (2) and (3) in Lemma B.3. Using (15) and (16), we obtain that, if $\ell(\alpha_3) \leq \ell(\alpha_2)$, then

$$\ell(p) = \tanh^{-1} \frac{\sinh \frac{\ell(\alpha_1)}{2}}{\frac{\cosh \frac{\ell(\alpha_3)}{2}}{\cosh \frac{\ell(\alpha_2)}{2}} + \cosh \frac{\ell(\alpha_1)}{2}} \geq \tanh^{-1} \frac{\sinh \frac{\ell(\alpha_1)}{2}}{1 + \cosh \frac{\ell(\alpha_1)}{2}} = \frac{\ell(\alpha_1)}{4}.$$

If $\ell(\alpha_2) < \ell(\alpha_3)$, using the inequality (14) and the assumption $\cosh \frac{\ell(\alpha_3)}{2} \leq 2$ we get

$$\ell(p) > \tanh^{-1}(\tanh([\frac{\cosh \frac{\ell(\alpha_2)}{2}}{\cosh \frac{\ell(\alpha_3)}{2}}]\frac{\ell(\alpha_1)}{4})) \gtrsim \ell(\alpha_1).$$

□

Appendix C

The sub-arc o_P of the geodesic arc between two boundary cuffs of a pair of pants of a decomposition of X in quadrilateral P lifts to the arc $[i, e^{\ell(o_P)}i]$ on the y-axis. Each point w in the lift $\tilde{P}$ of quadrilateral P belongs to the lift $\tilde{\gamma}_{w_0}$ of some geodesic arc γ_{w_0} orthogonal to o_P with foot w_0 on o_P. Note that $\tilde{\gamma}_{w_0}$ is a geodesic arc orthogonal to the y-axis and to its right. Map $\tilde{\gamma}_{w_0}$ by an isometry f to the Euclidean segment orthogonal to $[0, \ell(o_P)]$ and below the x-axis for each w_0 in o_P (see Figure 8.3). That completely defines f on $\tilde{P}$. We define f similarly on $\tilde{Q}$, $\tilde{R}$, and $\tilde{S}$. The definition of f is exactly the same as in Section 8.2.

Consider the inverse $g = f^{-1}$ of the diffeomorphism f defined on the lift $\tilde{P}$, $\tilde{Q}$, $\tilde{R}$, or $\tilde{S}$ of P, Q, R, or S in the front of a pair of pants Π. In this section we explain how g is quasiconformal with a quasiconformal constant that is bounded above by $k_0 = \frac{1+\operatorname{csch}^2(D)}{\coth(D)\operatorname{csch}(D)}$.

Proposition C.1. *The diffeomorphisms f from $\tilde{P}$, $\tilde{Q}$, $\tilde{R}$, and $\tilde{S}$ to $\mathbb{C}$ is quasiconformal with quasiconformal constant bounded above by $k_0 = \frac{1+\operatorname{csch}^2(D)}{\coth(D)\operatorname{csch}(D)}$.*

Proof. We obtain a diffeomorphism f from $\tilde{P}$ to $\mathbb{C}$ with quasiconformal constant bounded by k_0. Extend the result generally to every additional case. The inverse map g of f sends a point $z = x + iy$ to w such that $|w| = e^x$ and $\arg(w) = \tan^{-1}(\operatorname{csch}(-y))$. Thus, g is defined at $z = x + iy$ by

$$g(z) = f^{-1}(z) = e^x e^{i\tan^{-1}(\operatorname{csch}(-y))} = e^{\frac{z+\bar{z}}{2}} e^{i\tan^{-1}(\operatorname{csch}(\frac{\bar{z}-z}{2i}))}.$$

The dilatation of g at $z = x + iy$, denoted by $K(z)$, is

$$K(z) = \frac{1 + \operatorname{csch}^2(-y)}{\coth(-y)\operatorname{csch}(-y)}.$$

The value of $-y$ in $f(\tilde{P})$ is bounded above by $\ell(b_1)$, which is bounded above by a positive constant D (see Lemma B.3(1)). Note

$$\frac{1 + \operatorname{csch}^2(-y)}{\coth(-y)\operatorname{csch}(-y)}$$

is decreasing with respect to negative y. Thus, $g = f^{-1}$ is quasiconformal with quasiconformal constant bounded above by

$$k_0 = \frac{1 + \operatorname{csch}^2(D)}{\coth(D)\operatorname{csch}(D)}.$$

□

Bibliography

[1] S. Agard, *A geometric proof of Mostow's rigidity theorem for groups of divergence type.* Acta Math. 151 (1983), no. 3-4, 231-252.

[2] L. Ahlfors, *Lectures on Quasiconformal Mappings*, D. Van Nostrand Co., Inc., Ont., Toronto-New York-London, 1966.

[3] L. Ahlfors and L. Sario, *Riemann surfaces*, Princeton Mathematical Series, No. 26 Princeton University Press, Princeton, N.J. 1960.

[4] D. Alessandrini, L. Liu, A. Papadopoulos and W. Su, *On the inclusion of the quasiconformal Teichmüller space into the length-spectrum Teichmüller space*, Monatsh. Math. 179 (2016), no. 2, 165-189.

[5] K. Astala; M. Zinsmeister *Mostow rigidity and Fuchsian groups.* C. R. Acad. Sci. Paris Sér. I Math. 311 (1990), no. 6, 301-306.

[6] A. Basmajian, *Hyperbolic structures for surfaces of infinite type*, Trans. Amer. Math. Soc. 336 (1993), no. 1, 421-444.

[7] A. Basmajian, H. Hakobyan and D. Šarić, *The type problem for Riemann surfaces via Fenchel-Nielsen parameters*, Proc. Lond. Math. Soc. (3) 125 (2022), no. 3, 568-625.

[8] A. Basmajian and D. Šarić, *Geodesically complete hyperbolic structures*, Math. Proc. Cambridge Philos. Soc. 166 (2019), no. 2, 219-242.

[9] A. Beardon, *The geometry of discrete groups*, Graduate Texts in Mathematics, 159-161. Springer-Verlag, New York, 1983.

[10] C. Bishop, *Divergence groups have the Bowen property*, Ann. of Math. (2) 154 (2001), no. 1, 205-217.

[11] P. Buser, *Geometry and Spectra of Compact Riemann Surfaces*, Birkhäuser Boston, Ltd., Boston, MA; 2010.

[12] J. L. Fernández, M. V. Melián, *Escaping geodesics of Riemannian surfaces.* Acta Math. 187 (2001), no. 2, 213-236.

[13] C. McMullen, *Hausdorff dimension and conformal dynamics. III. Computation of dimension*, Amer. J. Math. 120 (1998), no. 4, 691-721.

[14] R. Nevanlinna, *Über die Existenz von beschränkten Potentialfunktionen auf Flächen von unendlichem Geschlecht.* (German) Math. Z. 52 (1950), 599-604.

[15] P. Nicholls, *The ergodic theory of discrete groups*, London Mathematical Society Lecture Note Series, 143. Cambridge University Press, Cambridge, 1989.

[16] I. Richards, *On the classification of noncompact surfaces*, Trans. Amer. Math. Soc. 106 (1963), 259-269.

[17] D. Šarić, *Circle homeomorphisms and shears*, Geom. Topol. 14 (2010), no. 4, 2405-2430.

[18] D. Šarić, *Quadratic differentials and foliations on infinite Riemann surfaces*, preprint, arXiv:2207.08626, to appear in Duke Math. J..

[19] H. Shiga, *On a distance defined by the length spectrum of Teichmüller space*, Ann. Acad. Sci. Fenn. Math. 28 (2003), no. 2, 315-326.

[20] D. Sullivan, *On the ergodic theory at infinity of an arbitrary discrete group of hyperbolic motions.* Riemann surfaces and related topics: Proceedings of the 1978 Stony

Brook Conference (State Univ. New York, Stony Brook, N.Y., 1978), pp. 465-496, Ann. of Math. Stud., 97, Princeton Univ. Press, Princeton, N.J., 1981.

[21] M. Tsuji, *Potential theory in modern function theory*, Reprinting of the 1959 original. Chelsea Publishing Co., New York, 1975.

[22] P. Tukia, *Differentiability and rigidity of Möbius groups.* Invent. Math. 82 (1985), no. 3, 557-578.